mechanisms of viral genome replication, we designed another comparative proteomic approach in which cells harboring genome-length bicistronic HCV RNA at the exponential growth phase (showing rapid replication of viral RNA) were compared with cells at the confluent-growth phase (showing poor replication of viral RNA). This strategy revealed that the chaperonin T-complex polypeptide (TCP1)-ring complex/chaperonin-containing TCP1 (TRiC/CCT) participates in HCV RNA replication and virion production possibly through an interaction between CCT5 (chaperonin-containing TCP1, subunit 5) and NS5B.

Results

CCT5 and Hsc70 are enriched in the DRM fraction containing the HCV RC

Recently, we analyzed the protein content of DRM fractions prepared from HCV subgenomic replicons and parental Huh-7 cells and identified 27 cellular proteins that were enriched in the DRM fraction prepared from the replicon cells (Hara et al., 2009). These were identified as factors that may be involved in the HCV RC and in viral replication. In fact, subsequent silencing of several genes coding for these proteins resulted in the inhibition of HCV RNA replication (Hara et al., 2009). However, it is likely that proteins unrelated to HCV replication are also included in the identified groups because long-term culture of the replicon cells under the selective pressure of G418 selects for a subpopulation of the parental cells and may induce changes in their protein expression profiles. Thus, to minimize interline differences in culture background, we further designed a comparative proteome analysis using a single cell line as follows.

HCV replication efficiency is dependent on the conditions of host cell growth. High cell density of the replicon culture has a reversible inhibitory effect on viral replication (Nelson and Tang, 2006; Pietschmann et al., 2001). Fig. 1A demonstrates that a high level of HCV RNA was detected in cells harboring the genome-length bicistronic HCV RNA, Con1 strain of genotype 1b (RCYM1) in the growth phase, whereas the RNA level declined sharply when the cells reached the stationary phase. We further compared the synthesis of HCV RNA in cell-free reaction mixtures containing the viral RC isolated from the RCYM1 cells at various cell densities (Fig. 1B). Replication activity was highest at the mid-log phase of cell growth (day 4 after seeding). By contrast, little or no RNA synthesis was observed under the confluent-growth cell culture (day 8), confirming the critical role of host cell growth conditions in the replication of the HCV genome.

Thus, to identify the host cell proteins required for HCV replication, we designed a two-dimensional fluorescence difference gel electrophoresis (2D-DIGE)-based comparative proteomics analysis of RC-rich DRM fractions prepared from RCYM1 cells at the mid-log and confluent-growth phases. Protein spots that reproducibly showed a greater than 1.5-fold difference in the mid-log growth- and the confluent phases were excised and digested by trypsin or lysylendopeptidase. Matrix-assisted laser desorption ionization–time-of-flight (MALDI-TOF) mass spectrometry (MS), which allows identification of the corresponding proteins in 9 cases (Table 1). Two increased spots that showed an increase in levels (their stereoscopic images are shown in Fig. 2A) were identified as CCT5 and Hsc70. CCT5, an epsilon subunit of chaperonin TRiC/CCT, is a 900-kDa toroid-shaped complex consisting of eight different subunits (Valpuesta et al., 2002; Yaffe et al., 1992). Hsc70, a member of the HSP70 family, is a 71-kDa heat shock cognate protein (Dworniczak and Mirault, 1987). Independent of the proteome analyses, DRM fractions and whole cell lysates were prepared from RCYM1 cells at two different growth phases (as above) and were analyzed by immunoblotting (Fig. 2B). Steady-state levels of CCT5 and Hsc70 were obviously higher in the DRM fraction prepared from the cells that were at the mid-log growth phase compared with those at the confluent phase. However, in the whole cell analyses, they were shown to be present at comparable levels during the two different growth phases. These results suggest that expression of CCT5 and Hsc70 is not enhanced in proliferating cells and that the enrichment of these proteins in the DRM fraction is possibly due to their post-translational modification. It should be noted that in the previous proteome analysis, CCT5 and other TRiC/CCT subunits, such as CCT1 and CCT2, were identified as proteins that were enriched in the DRM fraction prepared from subgenomic replicon-containing cells compared with that prepared from parental cells (Hara et al., 2009). We showed that CCT5 and CCT1 were enriched in the DRM fractions of cells transfected with the HCV genomic RNA derived from JFH-1 isolate as well as of subgenomic replicon cells (Fig. 2C).

TRiC/CCT participates in replication of the HCV genome

We investigated gain- and loss-of-functions of TRiC/CCT and Hsc70 with respect to the replication of HCV RNA. Seventy-two hours after RCYM1 cells were transfected with eight plasmids corresponding to each of the TRiC/CCT subunits, the level of HCV RNA in the cells (determined by quantitative RT-PCR) significantly increased to 2-fold that observed in the control cells. However, exogenous expression of Hsc70 in the RCYM1 cells showed no effect on the viral RNA (Fig. 3A). siRNAs targeted to CCT5 or Hsc70 and consisting of pools of three target-specific siRNAs or control nonspecific siRNAs were transfected

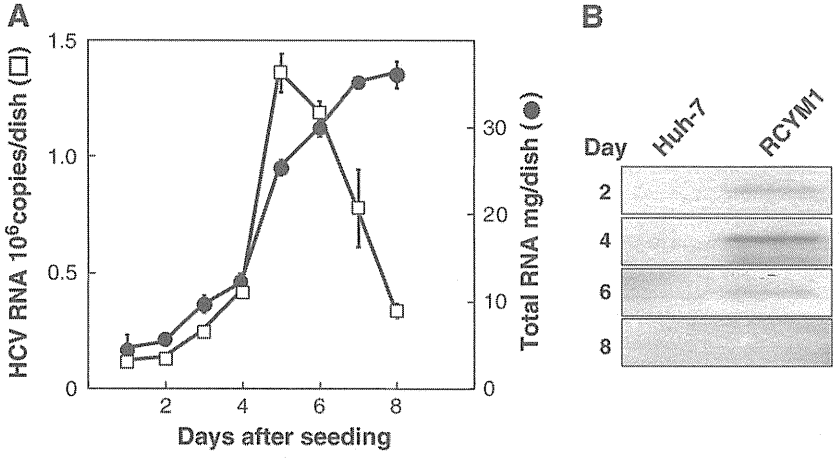

Fig. 1. Effect of cell growth on HCV RNA replication. (A) Measurement of HCV RNA (open squares) and total cellular RNA (closed circles) in RCYM1 cells at the time of harvest (days after seeding). (B) DRM fractions obtained from RCYM1 and parental Huh-7 cells harvested as indicated (day) were analyzed by cell-free RNA replication assay. RNA extracted from each sample was analyzed by agarose gel electrophoresis and autoradiograph.

Table 1
Selected cellular proteins that reproducibly increased and decreased in membrane fraction of RCYM1 cells at exponential growth phase.

Av. ratio	T-test	Coverage (%)	Protein name	Molecular function	GI
Increased proteins					
1.58	0.017	31	CCT5	Protein folding	33879913
1.54	0.005	35	HSPA8 (Hsc70)	Protein folding	24657660
Decreased proteins					
−1.95	0.028	44	Creatine kinase isozyme CK-B gene, exon 8	Energy pathway/metabolism	180568
−1.53	0.011	16	Chain C, Human Sirt2 Histone deacetylase	Cell cycle control	15826438
−2.14	0.001	33	Proteasome regulatory particle subunit p44S10	Metabolism	15341748
−1.71	0.004	21	Aldehyde dehydrogenase	Metabolism	178388
−1.85	0.004	40	Aminoacylase 1	Metabolism	12804328
−2.77	0.003	15	Eukaryotic translation initiation factor 3, subunit 3 gamma	Metabolism (translation regulator activity)	6685512
−2.43	0.014	20	Intraflagellar transport protein 74 homolog (Coiled-coil domain-containing protein 2)	Cell growth and/or maintenance	10439078

Three paired samples of RC-rich membrane fractions at the exponential- and confluent-growth phases of RCYM1 cultures were analyzed. The proteins representing a more than 1.5-fold increase or decrease (−) reproducibly and significantly are indicated.
Coverage (%): the ratio of the portion of protein sequence covered by matched peptides to the whole sequence.
GI: GenInfo Identifier number.

into RCYM1 cells. After 72 h, the HCV RNA level was reduced by 42% and 27% in the cells transfected with siRNAs against CCT5 and Hsc70, respectively, compared with controls (Fig. 3B). TRiC/CCT possibly interacts with Hsc70, and its complex formation contributes to increasing the efficiency of protein folding (Cuéllar et al., 2008). Our results suggest the involvement of TRiC/CCT and Hsc70 in the HCV life cycle. In particular, TRiC/CCT may play an important role in the replication of the viral genome.

To verify the specificity of the knockdown of CCT5 siRNA, we further synthesized two siRNAs targeted to different regions used in the above CCT5 siRNA and assessed their knockdown effect on HCV genome replication (Fig. 3C, upper panel). As expected, transfection of

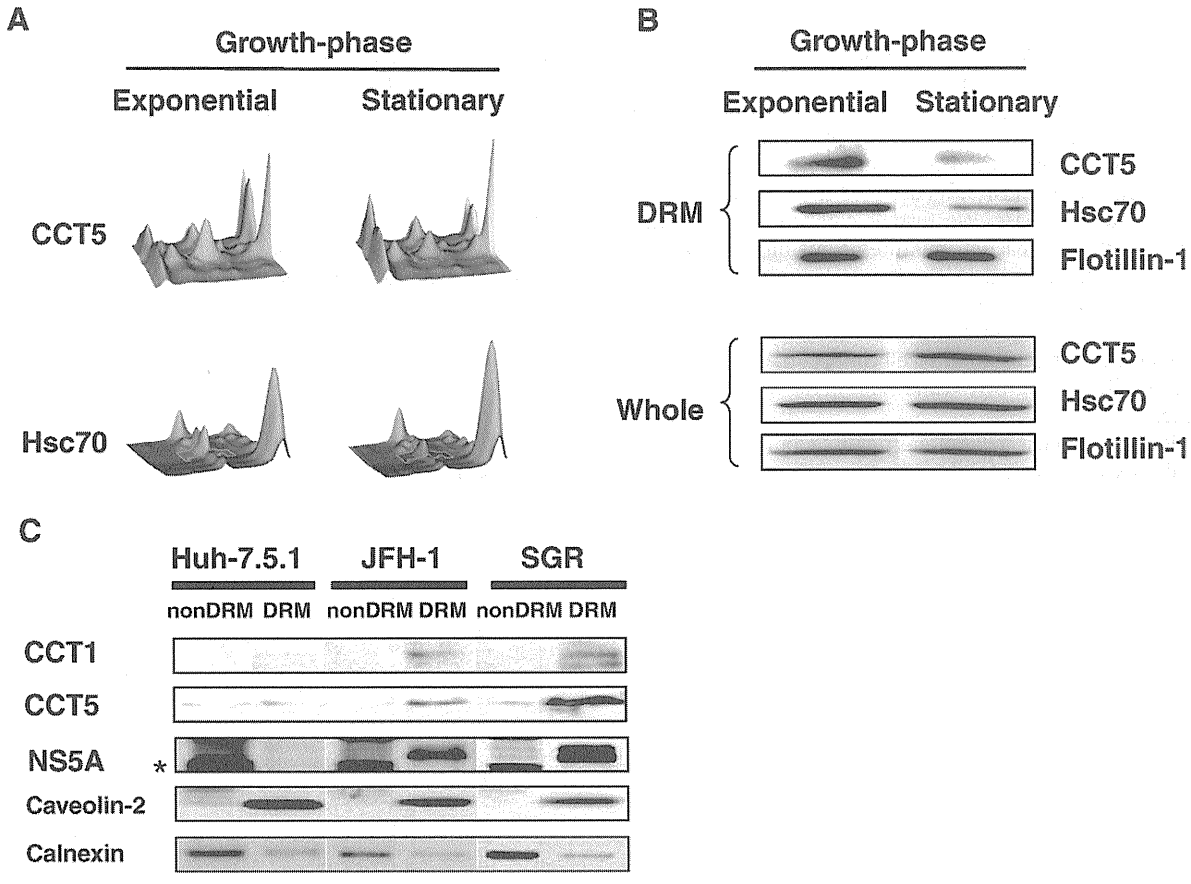

Fig. 2. Comparison of protein levels in DRM fractions prepared from RCYM1 cells at the exponential and stationary growth phases. (A) Three-dimensional images of CCT5 and Hsc70 analyzed by Ettan DIGE (GE Healthcare). Spots corresponding to CCT5/Hsc70 at exponential and stationary growth phases of the cells, respectively, are shown in green and red. (B) Equal amounts of protein in the DRM fractions prepared from RCYM1 cells at the exponential and stationary growth phases or corresponding whole cell lysates were analyzed by immunoblotting with Abs against CCT5, Hsc70 or flotillin-1. (C) Enrichment of CCT1 and CCT5 in the DRM fractions of HCV RNA replicating cells. Equal amounts of DRM or non-DRM fractions from full-length JFH-1 RNA transfected cells (JFH-1), subgenomic replicon cells (SGR) and parental Huh-7.5.1 cells were analyzed by immunoblotting with antibodies against CCT1, CCT5, NS5A, caveolin-2 or calnexin. *Non-specific bands.

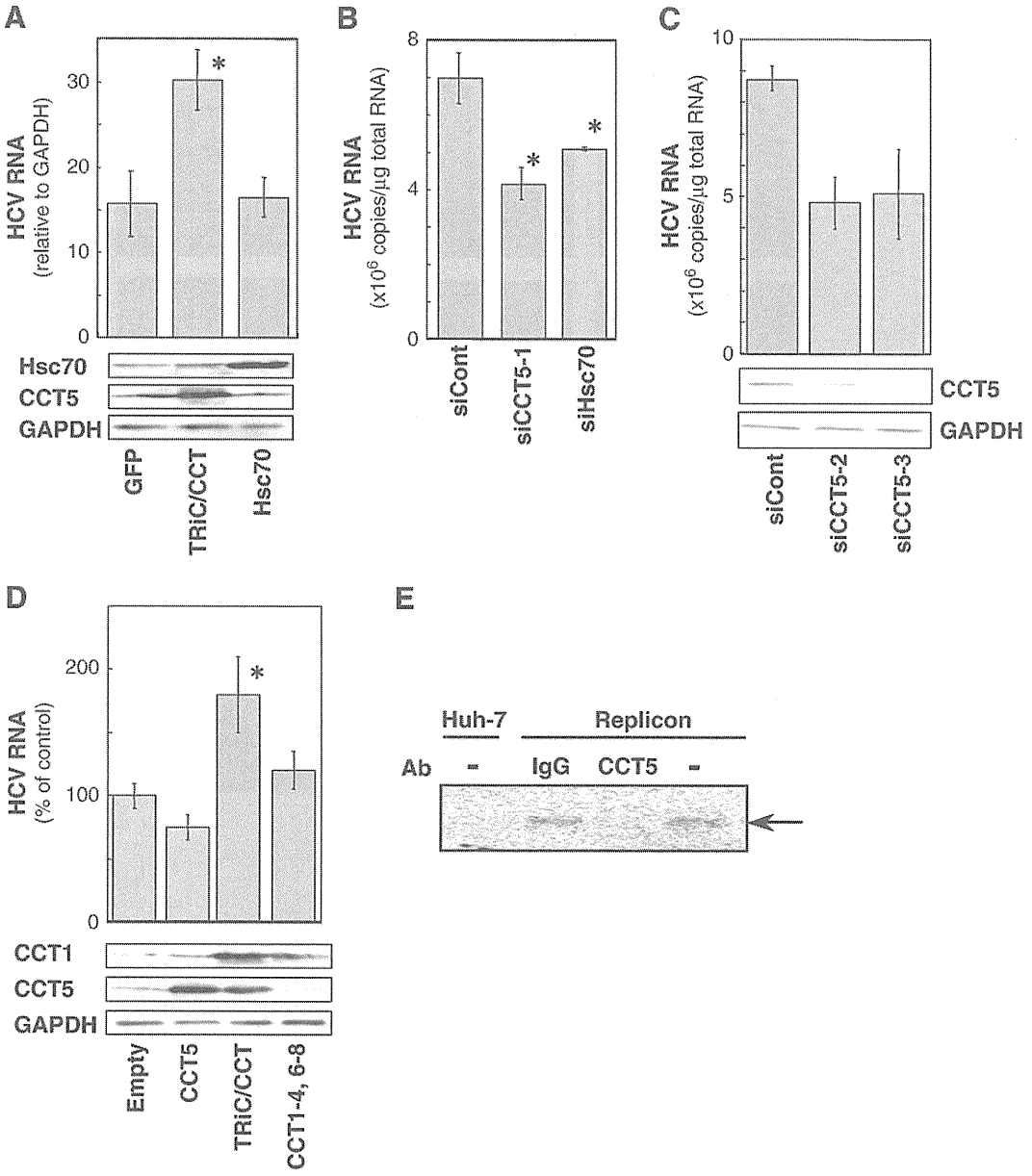

Fig. 3. Involvement of TRiC/CCT in HCV replication (A and D). Overexpression of all eight subunits of TRiC/CCT (TRiC/CCT); seven subunits, CCT1, 2, 3, 4, 6, 7, and 8 (CCT1–4, 6–8); subunit CCT5 only (CCT5); Hsc70; or control GFP in RCYM1 cells. HCV RNA levels were determined 48 h post-transfection (B and C). Knockdown of endogenous CCT5 or Hsc70 in RCYM1 cells, which were transfected with three types of siRNAs against CCT5 (siCCT5-1, -2, and -3), siRNA against Hsc70 (siHsc70), or control siRNA (siCont), and were harvested at 72 h post-transfection. siCCT5-1 and siHsc70 consisted of pools of three target-specific siRNAs. Immunoblotting for CCT1, CCT5, Hsc70 and GAPDH was performed (A, C and D; lower). (E) Cell-free de novo viral RNA synthesis assays were performed in the presence of anti-CCT5 Ab or control mouse IgG. Cytoplasmic fractions from SGR-N (replicon) and parental Huh-7 cells were used. An arrow indicates the synthesized HCV RNA. Error bars denote standard deviations with asterisks indicating statistical significance (*$P<0.01$).

RCYM1 cells with each CCT5 siRNA resulted in a reduction in viral RNA to a level of about 50% of that observed in cells treated with control siRNAs. Immunoblotting confirmed the efficient reduction in expression of endogenous CCT5 and the lack of cytotoxic effect exerted by the CCT5 siRNAs (Fig. 3C, middle and lower panels).

Having confirmed the upregulation of HCV RNA by ectopic expression of all the TRiC/CCT subunits, we further addressed the possibility that CCT5, independent of the complete TRiC/CCT complex, might have a role in promoting replication of HCV RNA. Transfection with either a CCT5 expression plasmid alone or with seven plasmids expressing all the TRiC/CCT subunits except CCT5 resulted in no or only a slight increase in the level of HCV RNA, indicating that all CCT subunits are required for HCV replication (Fig. 3D).

TRiC/CCT is generally known as a cytosolic chaperone (Valpuesta et al., 2002). However, it is enriched in the DRM fraction of HCV-replicating cells during the exponential growth phase (Fig. 2B). We used immunofluorescence staining to investigate whether TRiC/CCT is localized in the intracellular membrane compartments where replication of the viral genome occurs (Fig. 4). The de novo-synthesized RdRp was labeled by bromouridine triphosphate (BrUTP) incorporation in the presence of actinomycin D, and brominated nucleotides were detected with a specific antibody (Ab). Fluorescence staining in distinct speckles of various sizes was found in the cytoplasm of the HCV subgenomic replicon cells, whereas no signal was detected in the control cells, indicating that the observed BrUTP-incorporating RNA is mostly viral, newly synthesized viral RNA (Fig. 4A). Double immunofluorescence staining showed that a certain section of CCT5 co-distributed with the BrUTP-labeled RNA (Fig. 4A), which is known to co-exist with HCV NS proteins in viral replicating cells (Shi et al., 2003). We further observed that CCT5 was at least partially colocalized

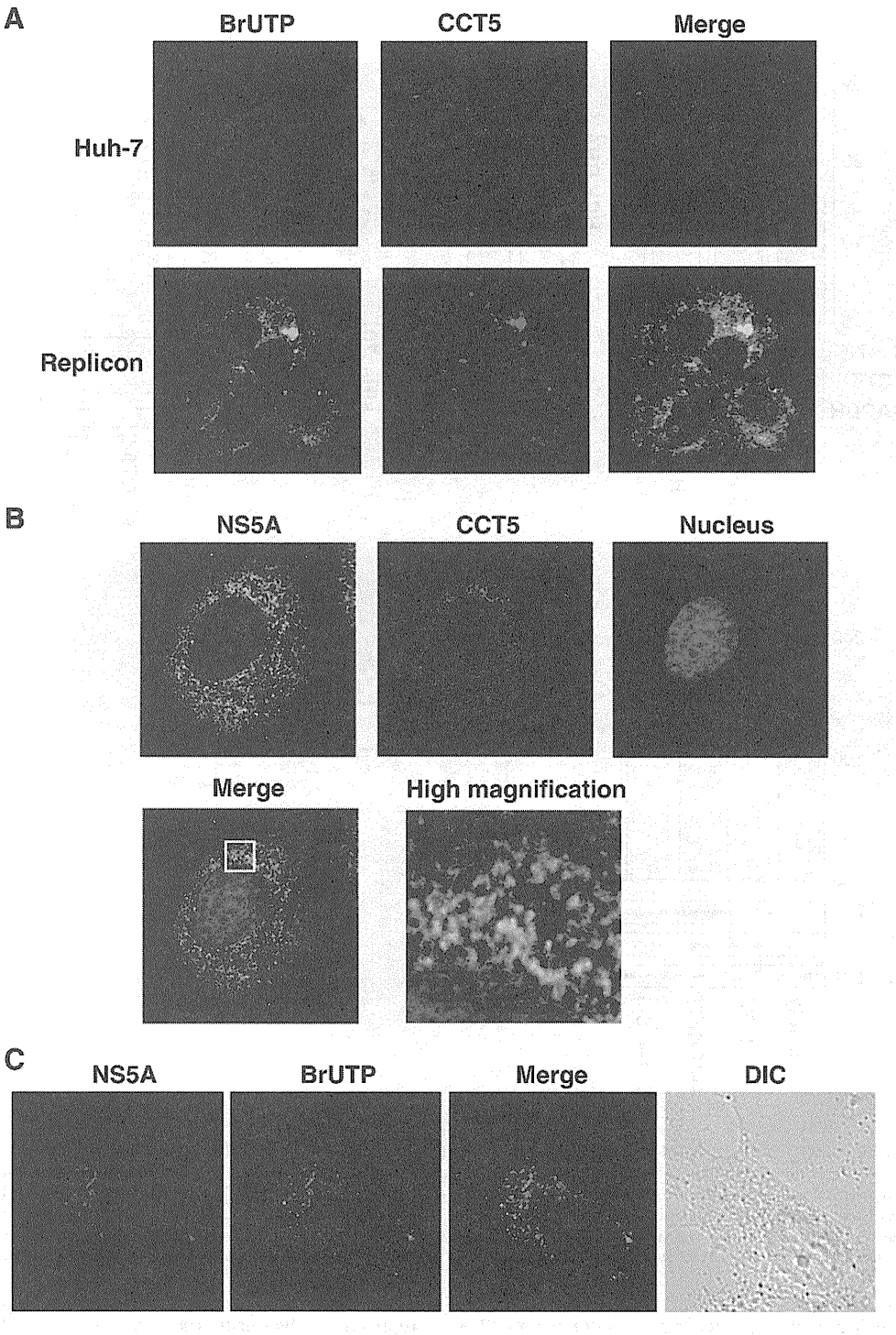

Fig. 4. Immunofluorescence analysis of CCT5 in SGR-N and Huh-7 cells (A) and HCVcc-infected cells (B). The primary Abs used were anti-CCT5 goat polyclonal Ab (red), anti-BrUTP monoclonal Ab (green), and anti-NS5A monoclonal Ab (green). Merged images of red and green signals (A) or of red, green and blue (nucleus) signals (B) are shown. The high magnification panel is an enlarged image of a white square of the merge panel. (C) Colocalization of NS5A protein with the viral RNA. The replicon cells were permeabilized with lysolecithin and labeled with BrUTP, followed by staining with anti-NS5A rabbit polyclonal Ab (red) and the anti-BrUTP monoclonal Ab (green). DIC, differential interference contrast.

with the viral NS protein in certain compartments sharing a dot-like structure in Huh-7 cells infected with HCV JFH-1 infectious HCV (HCVcc) derived from HCV genotype 2a (Fig. 4B) as well as in the replicon cells (data not shown). Fig. 4C indicated co-localization of BrUTP-labeled RNA with NS5A.

To further address the role of TRiC/CCT in HCV genome replication, we performed immunodepletion and in vitro replication analyses, which have been used for studying the genome replication of several viruses (Daikoku et al., 2006; Garcin et al., 1993; Liu et al., 2009). Cell extracts prepared from the HCV-replicating cells were reacted with either a mouse monoclonal Ab against CCT5 or mouse IgG derived from preimmune serum, followed by cell-free synthesis of HCV RNA. Fig. 3E shows that treatment with anti-CCT5 Ab inhibited viral RNA synthesis, whereas the control IgG did not affect the process, suggesting that TRiC/CCT participates directly in HCV RNA replication.

CCT5 interacts with HCV NS5B

The genome replication machinery of HCV is a membrane-associated complex composed of multiple factors including viral NS proteins. Given the involvement of TRiC/CCT in HCV RNA synthesis, we next examined its possible interaction with HCV NS proteins. A first attempt to immunoprecipitate the viral proteins with antibodies against TRiC/CCT subunits in the replicon cells was unsuccessful (data not shown), suggesting that endogenous levels of TRiC/CCT is not sufficient to pull out NS5B. Next, dual (myc/FLAG)-tagged NS3, NS5A, or NS5B proteins derived from the genotype 1b NIHJ1 strain were co-expressed with CCT5 in Huh-7 cells and then subjected to two-step immunoprecipitation with anti-myc and anti-FLAG Abs (Ichimura et al., 2005; Shirakura et al., 2007). An empty plasmid was used as a negative control in the analyses. As shown in Fig. 5A, CCT5 specifically interacted with NS5B. Little or no interaction was found between CCT5 and NS3 or NS5A. To determine the NS5B region required for the interaction with CCT5, various deletion mutants of HA-NS5B were constructed and their interactions with CCT5 were analyzed as described above. CCT5 was shown to be coimmunoprecipitated with either a full-length NS5B (aa 1–591), an N-terminal deletion (aa 71–591) or a C-terminal deletion (aa 1–570), but not with deletions aa 215–591 or aa 320–591 (Fig. 5B), suggesting that aa 71–214 of NS5B are important for its interaction with CCT5.

Knockdown of CCT5 results in the reduction of propagation of infectious HCV

We further examined whether the knockdown of CCT5 would abrogate the production of infectious HCV (HCVcc), derived from JFH-1 (Fig. 6). At 72 h post-transfection with each CCT5 siRNA, HCV RNA

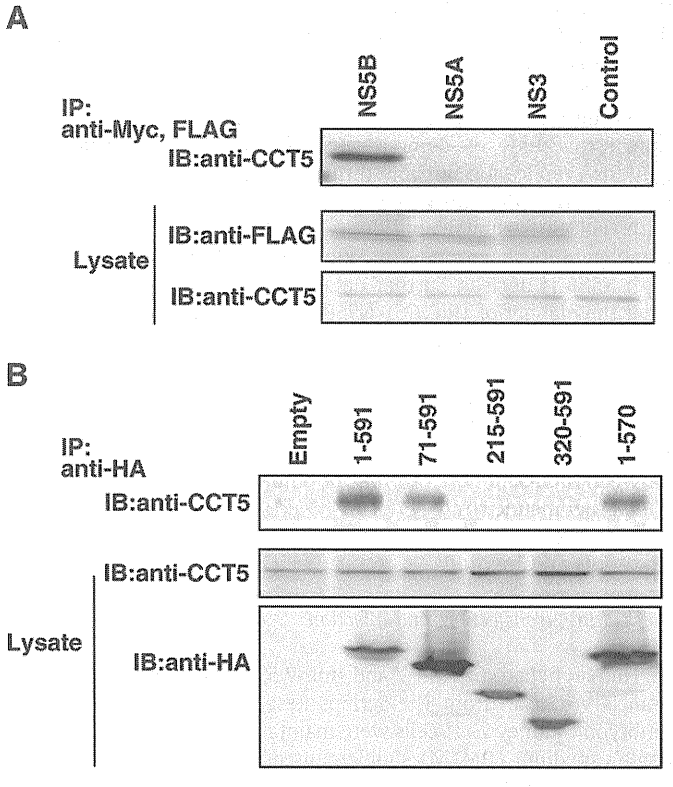

Fig. 5. CCT5 interacts with HCV NS5B. (A) CCT5 was co-expressed with MEF-tagged-NS5B, -NS5A, or -NS3 protein of strain NIHJ1 in cells, followed by two-step immunoprecipitation (IP) with anti-FLAG and anti-myc Abs. Immunoprecipitates were subjected to immunoblotting with anti-CCT5 Ab (IB). (B) Full-length NS5B (1–591) or its deletions (71–591, 215–591, 320–591, 1–570) along with a HA tag were co-expressed with CCT5. IP and IB were performed as described above.

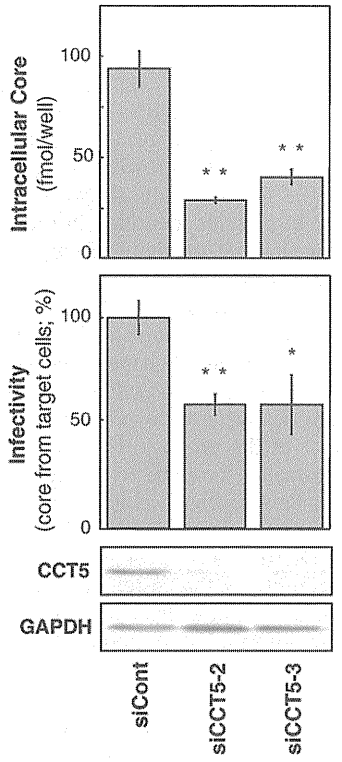

Fig. 6. Knockdown of endogenous CCT5 in HCVcc-infected cells. The cells were transfected with siRNAs against CCT5 (siCCT5-2, -3) or with control siRNAs (siCont). At 72 h post-transfection, the viral core protein levels in cells were determined (upper panel). Collected culture supernatants were inoculated into naïve Huh7.5.1 cells and intracellular core proteins were determined at 72 h post-infection (middle panel). Cells transfected with siRNAs were analyzed by immunoblotting with anti-CCT5 or anti-GAPDH Ab (lower panel). Error bars denote standard deviations with asterisks indicating statistical significance (*$P<0.05$; **$P<0.01$).

levels in Huh-7 cells infected with HCVcc were reduced by 25–35% compared with controls. Accordingly, virion production from CCT5 siRNA-transfected cultures was significantly decreased, as determined by intracellular HCV core protein levels at 72 h after the infection of naïve cells with culture supernatants taken from transfected cells. These results demonstrate that reduction of the HCV RNA replication by siRNA-mediated knockdown of CCT5 results in reduction of the propagation of the infectious virus.

Discussion

The chaperone-assisted protein-folding pathway is a process in living cells that results from coordinated interactions between multiple proteins that often form multi-component complexes. Several steps in the viral life cycle, such as protein processing, genome replication, and viral assembly, are regulated by cellular chaperones. Hsp90, one of the most abundant proteins in unstressed cells, has been implicated in HCV RNA replication (Nakagawa et al., 2007; Okamoto et al., 2006, 2008; Taguwa et al., 2008, 2009; Ujino et al., 2009). FKBP8, a member of the FKBP506-binding protein family, and hB-ind1, human butyrate-induced transcript 1, play key roles through their interaction with HCV NS5A and Hsp90 (Okamoto et al., 2006, 2008; Taguwa et al., 2008, 2009). Hsp90 has also been implicated in viral enzymatic activities including those of the influenza virus (Momose et al., 2002; Naito et al., 2007), herpes simplex virus (Burch and Weller, 2005), Flock house virus (Kampmueller and Miller, 2005), and hepatitis B virus (Hu et al., 2004).

In our former study, comparative proteome analyses of the viral RC-rich DRM fractions prepared from subgenomic replicon cells and Huh-7 cells were carried out to identify host factors involved

in HCV replication (Hara et al., 2009). We extended the proteomics by modifying our protocol of the analysis to reduce the interline differences in culture background and analyzed the DRM samples derived from the mid-log and confluent-growth phases of single cell line. Here, we identified two proteins, CCT5 and Hsc70, showing an increase in levels at the mid-log growth phase. Although CCT5 was also identified in the former study as expected, Hsc70 was not included in the list of proteins identified in the study (Hara et al., 2009). This difference may be due to the use of cells carrying the full-length replicon RNA in this study.

In this study, we demonstrated that TRiC/CCT participates in HCV RNA replication and virion production possibly through its interaction with NS5B. TRiC/CCT is a group II chaperonin that assists in protein folding in eukaryotic cells and forms a double-ring-like hexadecamer complex. Although relatively little is known about its function compared with that of the group I chaperonins such as bacterial GroEL, several mammalian proteins whose folding is mediated by TRiC/CCT have been identified, such as actin, tubulin, and von Hippel–Lindau tumor suppressor protein (Farr et al., 1997; Feldman et al., 2003; Frydman and Hartl, 1996; Meyer et al., 2003; Tian et al., 1995). With regard to viral proteins, the Epstein–Barr virus nuclear antigen, HBV capsid protein, and p4 of M-PMV have been identified as TRiC/CCT-interacting proteins (Yam et al., 2008). However, the functional significance of their interactions in the viral life cycles has yet to be determined. Here we demonstrated that the reduction in CCT5 expression in HCV replicon cells and in virus-infected cells inhibits HCV RNA replication (Figs. 3B and C) and virus production (Fig. 6) respectively. Gain-of-function was also shown by co-transfection of the replicon cells with eight constructs corresponding to all the TRiC/CCT subunits (Figs. 3A and D).

A recent study of the three-dimensional structure of the TRiC/CCT and Hsc70 complex has demonstrated that the apical domain of the CCT2 (CCT-beta) subunit is involved in the interaction with Hsc70 (Cuéllar et al., 2008). The complex formation created by the TRiC/CCT and Hsc70 interaction may promote higher efficiency in the folding of certain proteins (Cuéllar et al., 2008). In our comparative proteome analyses, both CCT subunits and Hsc70 were enriched in the HCV RC-rich membrane fraction of the replicon cells that showed high viral replication activity (Fig. 2B). Transfection of Hsc70 siRNA into the replicon cells moderately inhibited viral RNA replication (Fig. 3B). However, upregulation of HCV replication was not observed by ectopic expression of Hsc70 (Fig. 3A), and little or no interaction was observed between Hsc70 and HCV NS proteins in the co-immunoprecipitation analysis (data not shown). Thus, it is likely that TRiC/CCT acts as a regulator of HCV replication through participating in the de novo folding of NS5B RdRp, and Hsc70 might serve to assist in folding through its interaction with TRiC/CCT. It was recently reported that Hsc70 is associated with HCV particles and modulates the viral infectivity (Parent et al., 2009). Here we showed an additional role of Hsc70 in the HCV life cycle.

HCV genomic single-stranded RNA serves as a template for the synthesis of the full-length minus strand that is used for the overproduction of the virus-specific genomic RNA. NS5B RdRp is a single subunit catalytic component of the viral replication machinery responsible for both of these processes. It is known that the in vitro RdRp activity of recombinant NS5B expressed in and purified from insect cells and *Escherichia coli* is low in many cases. This could be due to the lack of a suitable cellular environment for favorable RdRp activity, although the particular conformational features dependent on the viral isolates may also be involved (Lohmann et al., 1997; Weng et al., 2009). In fact, besides interacting with HCV NS proteins, NS5B has been reported to interact with several host cell proteins. For example, human vesicle-associated membrane protein-associated protein subtype A (VAP-A) and subtype B (VAP-B), which are involved in the regulation of membrane trafficking, lipid transport and metabolism, and the unfolded protein response, interact with NS5B and NS5A and participate in HCV replication (Hamamoto et al., 2005). Recently, VAP-C, a splicing variant of VAP-B, was found to act as a negative regulator of viral replication through its interaction with NS5B but not with VAP-A (Kukihara et al., 2009). Cyclophilin A and B, peptidyl-prolyl isomerases that facilitate protein folding by catalyzing the *cis–trans* interconversion of peptide bonds at proline residues, play a role in stimulating HCV RNA synthesis through interaction with NS5B (Liu et al., 2009; Watashi et al., 2005). SNARE-like protein (Tu et al., 1999), eIF4AII (Kyono et al., 2002), protein kinase C-related kinase 2 (Kim et al., 2004), nucleolin (Kim et al., 2004; Hirano et al., 2003; Shimakami et al., 2006), and p68 (Goh et al., 2004) are also known to associate with NS5B and are possibly involved in HCV RNA replication.

We found that the aa 71–214 region in NS5B is important for interaction with TRiC/CCT. The catalytic domain of HCV RdRp has a "right-hand" configuration similar to other viral polymerases, such as HIV-1 reverse transcriptase (Huang et al., 1998) and poliovirus RdRp (Hansen et al., 1997), and is divided into the fingers, palm, and thumb functional subdomains (Lohmann et al., 2000). The region required for the interaction with TRiC/CCT has been mapped in a part of the fingers and palm domains of NS5B RdRp. To address how TRiC/CCT assists in the correct folding or disaggregation of NS5B through their interaction, leading to the formation of a functional RdRp, work based on an in vitro reconstitution system using purified proteins is under way. As all the TRiC/CCT subunits possess essentially identical ATPase domains, their protein-recognition regions are apparently divergent, allowing for substrate-binding specificity. It has recently been reported that TRiC/CCT interacts with the PB2 subunit of the influenza virus RNA polymerase complex and TRiC/CCT binding site is located in the central region of PB2, suggesting involvement of TRiC/CCT in the influenza virus life cycle (Fislová et al., 2010). Eukaryotic RNA polymerase subunit has also been identified as a binding partner of TRiC/CCT from interactome analysis (Yam et al., 2008). It would be interesting to examine how conserved the mechanisms of TRiC/CCT action that result in enhanced replication are among RNA polymerases.

The recruitment of a chaperonin by viral NS proteins may be important for understanding regulation of the viral genome replication. In this study, we demonstrated the involvement of TRiC/CCT in HCV RNA replication possibly through its interaction between TRiC/CCT and HCV NS5B. Although possible interaction of subunit CCT5 with NS5B was shown, considering involvement of whole TRiC/CCT complex in its chaperonin function, whether CCT5 directly interacts with NS5B is unclear. Further detailed studies are needed to make clear the manner of TRiC/CCT-NS5B interaction. NS5B RdRp is one of the main targets for HCV drug discovery. The search for NS5B inhibitors has resulted in the identification of several binding sites on NS5B, such as the domain adjacent to the active site and the allosteric GTP site (De Francesco and Migliaccio, 2005; Laporte et al., 2008). The findings obtained here suggest that disturbing the interaction between NS5B and TRiC/CCT may be a novel approach for an antiviral chemotherapeutic strategy.

Materials and methods

Cell culture, transfection, and infection

Human hepatoma Huh-7 and Huh-7.5.1 cells (kindly provided by Francis V. Chisari from The Scripps Research Institute) and human embryonic kidney 293T cells were maintained in Dulbecco's modified Eagle's medium (DMEM) supplemented with 10% fetal calf serum. Huh-7-derived SGR-N (Shi et al., 2003) and RCYM1 (Murakami et al., 2006) cells, which possess subgenomic replicon RNA from the HCV-N strain (Guo et al., 2001; Ikeda et al., 2002) and genome-length HCV RNA from the Con 1 strain (Pietschmann et al., 2002), were cultured in the above medium in the presence of 1 mg/ml G418. Cells were transfected with plasmid DNAs using FuGENE transfection reagents

(Roche Diagnostics, Tokyo, Japan). Culture media from Huh-7 cells transfected with in vitro-transcribed RNA corresponding to the full-length HCV RNA derived from the JFH-1 strain (Wakita et al., 2005) were collected, concentrated, and used for the infection assay (Aizaki et al., 2008).

Ab

Primary Abs used in this study were mouse monoclonal Abs against FLAG (Sigma-Aldrich, St. Louis, MO), c-myc (Sigma-Aldrich), CCT5 (Abnova Corporation, Taipei City, Taiwan), flotillin-1 (BD Biosciences, San Jose, CA), glyceraldehyde-3-phosphate dehydrogenase (GAPDH) (Chemicon, Temecula, CA), BrdU (Caltag, CA) and HCV NS5A (Austral Biologicals, San Ramon, CA), a rabbit polyclonal Ab against hemagglutinin (HA; Sigma-Aldrich), a sheep polyclonal Ab against bromodeoxyuridine (Biodesign International, Saco, ME), and goat polyclonal Abs against the individual subunits of CCT (Santa Cruz Biotechnology, Santa Cruz, CA) and Hsc70 (Santa Cruz Biotechnology). Anti Hsc70 and CCT5 monoclonal rat Abs were obtained from Abcam (Tokyo, Japan) and AbD serotec (Oxford, UK). Rabbit polyclonal antibody to NS5A was described previously (Hamamoto et al., 2005). Anti NS5B monoclonal Ab was kindly provided by D. Moradpour (Centre Hospitalier Universitaire Vaudois, University of Lausanne; Moradpour et al., 2002).

Plasmids

To generate expression plasmids for the NS proteins with dual epitope tags, DNA fragments encoding the NS3, NS5A, or NS5B proteins were amplified from HCV strain NIHJ1 (Aizaki et al., 1998) by PCR and cloned into the EcoRI–EcoRV sites of pcDNA3-MEF, which includes the MEF tag cassette containing the *m*yc tag, TEV protease cleavage site, and FLAG tag sequences (Ichimura et al., 2005; Shirakura et al., 2007). To create a series of NS5B truncation mutants, each fragment was amplified by PCR and cloned into the EcoRI–XhoI site of pCMV-HA (Clontech, Mountain View, CA). To generate expression plasmids for the individual CCT subunits, cDNA fragments encoding human CCT1 through CCT8 were amplified from the total cellular RNA by RT-PCR and then cloned into the SmaI site of pCAGGS (Niwa et al., 1991). All PCR products were confirmed by nucleotide sequencing.

Proteome analysis

RC-rich membrane fractions from the cells were isolated as described previously (Aizaki et al., 2004). Briefly, cells were lysed in hypotonic buffer. After removing the nuclei, the supernatants were mixed with 70% sucrose, overlaid with 55% and 10% sucrose, and centrifuged at 38,000 rpm for 14 h. Proteins from the membrane fractions were then analyzed by 2D-DIGE as described previously (Hara et al., 2009). Briefly, protein samples were resolved in protein solubilization buffer (Bio-Rad Laboratories, Tokyo, Japan) and washed with pH adjustment buffer (7 M urea, 2 M thiourea, 4% CHAPS, 30 mM Tris–HCl [pH 10.0]), before being labeled with fluorescent dyes; the dyes used were Cy3 for RCYM1 cells samples taken at the exponential growth phase, Cy5 for cells samples taken at the confluent phase, and Cy2 for a protein standard containing equal amounts of both cell samples. Aliquots of the labeled samples were pooled and applied to Immobiline DryStrip (GE Healthcare, Tokyo, Japan) for first-dimension separation and to 12.5% polyacrylamide gels for second-dimension separation. Images of the 2-D gels were captured on a Typhoon scanner (GE Healthcare), and analyzed quantitatively using DeCyder v5.0 software (GE Healthcare). Samples were analyzed in triplicate as independent cultures and the Student's *t*-test was applied using the DeCyder biological variation analysis module to validate the significance of the differences in spot intensity detected between the samples.

In vitro RNA replication assay

In vitro replication of HCV RNA was performed as described previously (Hamamoto et al., 2005). Briefly, cytoplasmic fractions of subgenomic replicon cells were treated with 1% NP-40 at 4 °C for 1 h, followed by being incubated with 1 mM of ATP, GTP, and UTP; 10 μM CTP; [^{32}P]CTP (1 MBq; 15 TBq/mmol); 10 μg/ml actinomycin D; and 800 U/ml RNase inhibitor (Promega, Madison, WI) for 4 h at 30 °C. RNA was extracted from the total mixture by using TRI Reagent (Molecular Research Center, Cincinnati, OH). The RNA was precipitated, eluted in 10 μl of RNase-free water, and analyzed by 1% formaldehyde-agarose gel electrophoresis. For the immunodepletion assay, the cytoplasmic fractions were incubated with anti-CCT5 Ab in the presence of NP-40 for 4 h before NTP incorporation.

MALDI-TOF MS analysis

Target spots were cut and collected from gels under UV luminescence and rechecked with Typhoon scanner. The spot gels of the target proteins were subjected to in-gel trypsin digestion and analyzed by MALDI-TOF MS meter (Voyager-DE STR, Applied Biosystems, Tokyo, Japan) as described previously (Yanagida et al., 2000). All proteins were identified by peptide mass fingerprinting.

Immunoblot analysis and immunoprecipitation

Immunoblot analysis was performed essentially as described previously (Aizaki et al., 2004). The membrane was visualized with SuperSignal West Pico chemiluminescent substrate (Pierce, Rockford, IL). For immunoprecipitation, cells transfected with plasmids expressing epitope-tagged HCV protein or CCT5 were lysed and then subjected to two-step precipitations with anti-myc and anti-FLAG Abs according to the procedures described previously (Ichimura et al., 2005). In some experiments, HA-tagged full-length NS5B (aa 1–591) or its deletion mutants (aa 71–591, 215–591, 320–591, 1–570) were co-expressed with CCT5 in cells, followed by single-step immunoprecipitation and immunoblotting.

Immunofluorescence staining

Cell permeabilization with lysolecithin and detection of de novo-synthesized viral RNA was performed as described previously (Shi et al., 2003). Briefly, Huh-7 cells were plated on 8-well chamber slides at a density of 5×10^4 cells per well. Cells were incubated with actinomycin D (5 μg/μl) for 1 h and were washed twice with serum-free medium, before being incubated for 10 min on ice. The cells were then incubated in a transcription buffer containing 0.5 mM BrUTP for 30 min. The cells were fixed in 4% formaldehyde for 20 min and then incubated for 15 min in 0.1% Triton X-100 in phosphate-buffered saline (PBS). Primary Abs were diluted in 5% bovine serum albumin in PBS and were incubated with the cells for 1 h. After washing with PBS, fluorescein-conjugated secondary Abs (Jackson Immunoresearch Laboratories, West Grove, PA) were added to the cells at a 1:200 dilution for 1 h. The slides were then washed with PBS and mounted in ProLong Antifade (Molecular Probes, Eugene, OR). Confocal microscopy was performed on a Zeiss Confocal Laser Scanning Microscope LSM 510 (Carl Zeiss MicroImaging, Thornwood, NY).

RNA interference

Small interfering RNAs (siRNAs) targeted to CCT5 or Hsc70 and scrambled negative control siRNAs were purchased from Sigma-Aldrich Japan (Tokyo, Japan). Cells were plated on a 24-well plate with

antibiotic-free DMEM overnight, and each plate was transfected with 10 nM siRNAs by X-tremeGENE (Roche Diagnostics) according to the manufacturer's protocol. Forty-eight hours post-transfection, the total RNA and protein extracts were prepared and subjected to real-time RT-PCR and immunoblot analyses, respectively.

Quantitation of HCV RNA and core protein

Total RNA was extracted from cells using TRIzol reagent (Invitrogen, Carlsbad, CA) according to the manufacturer's instructions. Real-time RT-PCR was performed using TaqMan EZ RT-PCR Core Reagents (PE Applied Biosystems, Foster City, CA) as described previously (Aizaki et al., 2004; Murakami et al., 2006). HCV core protein levels in the cells and in the supernatant were quantified using an HCV core enzyme-linked immunosorbent assay (Ortho-Clinical Diagnostics, Tokyo, Japan).

Acknowledgments

We thank Drs. F. V. Chisari (The Scripps Research Institute) and D. Moradpour (Centre Hospitalier Universitaire Vaudois, University of Lausanne) for providing the Huh-7.5.1 cells and anti-NS5B monoclonal antibody, respectively; S. Yoshizaki, M. Kaga, M. Sasaki, and T. Date for their technical assistance, and T. Mizoguchi for secretarial work. This work was supported by a grant-in-aid for Scientific Research from the Japan Society for the Promotion of Science, from the Ministry of Health, Labour and Welfare of Japan, and from the Ministry of Education, Culture, Sports, Science and Technology, and by Research on Health Sciences focusing on Drug Innovation from the Japan Health Sciences Foundation, and by the Program for Promotion of Fundamental Studies in Health Sciences of the National Institute of Biomedical Innovation of Japan.

References

Aizaki, H., Aoki, Y., Harada, T., Ishii, K., Suzuki, T., Nagamori, S., Toda, G., Matsuura, Y., Miyamura, T., 1998. Full-length complementary DNA of hepatitis C virus genome from an infectious blood sample. Hepatology 27 (2), 621–627.

Aizaki, H., Lee, K.J., Sung, V.M., Ishiko, H., Lai, M.M., 2004. Characterization of the hepatitis C virus RNA replication complex associated with lipid rafts. Virology 324 (2), 450–461.

Aizaki, H., Morikawa, K., Fukasawa, M., Hara, H., Inoue, Y., Tani, H., Saito, K., Nishijima, M., Hanada, K., Matsuura, Y., Lai, M.M., Miyamura, T., Wakita, T., Suzuki, T., 2008. Critical role of virion-associated cholesterol and sphingolipid in hepatitis C virus infection. J. Virol. 82 (12), 5715–5724.

Ali, N., Tardif, K.D., Siddiqui, A., 2002. Cell-free replication of the hepatitis C virus subgenomic replicon. J. Virol. 76 (23), 12001–12007.

Burch, A.D., Weller, S.K., 2005. Herpes simplex virus type 1 DNA polymerase requires the mammalian chaperone hsp90 for proper localization to the nucleus. J. Virol. 79 (16), 10740–10749.

Cuéllar, J., Martín-Benito, J., Scheres, S.H., Sousa, R., Moro, F., López-Viñas, E., Gómez-Puertas, P., Muga, A., Carrascosa, J.L., Valpuesta, J.M., 2008. The structure of CCT-Hsc70 NBD suggests a mechanism for Hsp70 delivery of substrates to the chaperonin. Nat. Struct. Mol. Biol. 15 (8), 858–864.

Daikoku, T., Kudoh, A., Sugaya, Y., Iwahori, S., Shirata, N., Isomura, H., Tsurumi, T., 2006. Postreplicative mismatch repair factors are recruited to Epstein–Barr virus replication compartments. J. Biol. Chem. 281 (16), 11422–11430.

De Francesco, R., Migliaccio, G., 2005. Challenges and successes in developing new therapies for hepatitis C. Nature 436 (7053), 953–960.

Dworniczak, B., Mirault, M.E., 1987. Structure and expression of a human gene coding for a 71 kd heat shock 'cognate' protein. Nucleic Acids Res. 15 (13), 5181–5197.

Farr, G.W., Scharl, E.C., Schumacher, R.J., Sondek, S., Horwich, A.L., 1997. Chaperonin-mediated folding in the eukaryotic cytosol proceeds through rounds of release of native and nonnative forms. Cell 89 (6), 927–937.

Feldman, D.E., Spiess, C., Howard, D.E., Frydman, J., 2003. Tumorigenic mutations in VHL disrupt folding in vivo by interfering with chaperonin binding. Mol. Cell 12 (5), 1213–1224.

Fislová, T., Thomas, B., Graef, K.M., Fodor, E., 2010. Association of the influenza virus RNA polymerase subunit PB2 with the host chaperonin CCT. J. Virol. 84 (17), 8691–8699.

Frydman, J., Hartl, F.U., 1996. Principles of chaperone-assisted protein folding: differences between in vitro and in vivo mechanisms. Science 272 (5267), 1497–1502.

Garcin, D., Rochat, S., Kolakofsky, D., 1993. The Tacaribe arenavirus small zinc finger protein is required for both mRNA synthesis and genome replication. J. Virol. 67 (2), 807–812.

Goh, P.Y., Tan, Y.J., Lim, S.P., Tan, Y.H., Lim, S.G., Fuller-Pace, F., Hong, W., 2004. Cellular RNA helicase p68 relocalization and interaction with the hepatitis C virus (HCV) NS5B protein and the potential role of p68 in HCV RNA replication. J. Virol. 78 (10), 5288–5298.

Guo, J.T., Bichko, V.V., Seeger, C., 2001. Effect of alpha interferon on the hepatitis C virus replicon. J. Virol. 75 (18), 8516–8523.

Hamamoto, I., Nishimura, Y., Okamoto, T., Aizaki, H., Liu, M., Mori, Y., Abe, T., Suzuki, T., Lai, M.M., Miyamura, T., Moriishi, K., Matsuura, Y., 2005. Human VAP-B is involved in hepatitis C virus replication through interaction with NS5A and NS5B. J. Virol. 79 (21), 13473–13482.

Hansen, J.L., Long, A.M., Schultz, S.C., 1997. Structure of the RNA-dependent RNA polymerase of poliovirus. Structure 5 (8), 1109–1122.

Hara, H., Aizaki, H., Matsuda, M., Shinkai-Ouchi, F., Inoue, Y., Murakami, K., Shoji, I., Kawakami, H., Matsuura, Y., Lai, M.M., Miyamura, T., Wakita, T., Suzuki, T., 2009. Involvement of creatine kinase B in hepatitis C virus genome replication through interaction with the viral NS4A protein. J. Virol. 83 (10), 5137–5147.

Hardy, R.W., Marcotrigiano, J., Blight, K.J., Majors, J.E., Rice, C.M., 2003. Hepatitis C virus RNA synthesis in a cell-free system isolated from replicon-containing hepatoma cells. J. Virol. 77 (3), 2029–2037.

Hirano, M., Kaneko, S., Yamashita, T., Luo, H., Qin, W., Shirota, Y., Nomura, T., Kobayashi, K., Murakami, S., 2003. Direct interaction between nucleolin and hepatitis C virus NS5B. J. Biol. Chem. 278 (7), 5109–5115.

Hoofnagle, J.H., 2002. Course and outcome of hepatitis C. Hepatology 36 (5 Suppl 1), S21–S29.

Hu, J., Flores, D., Toft, D., Wang, X., Nguyen, D., 2004. Requirement of heat shock protein 90 for human hepatitis B virus reverse transcriptase function. J. Virol. 78 (23), 13122–13131.

Huang, H., Chopra, R., Verdine, G.L., Harrison, S.C., 1998. Structure of a covalently trapped catalytic complex of HIV-1 reverse transcriptase: implications for drug resistance. Science 282 (5394), 1669–1675.

Ichimura, T., Yamamura, H., Sasamoto, K., Tominaga, Y., Taoka, M., Kakiuchi, K., Shinkawa, T., Takahashi, N., Shimada, S., Isobe, T., 2005. 14-3-3 proteins modulate the expression of epithelial Na+ channels by phosphorylation-dependent interaction with Nedd4-2 ubiquitin ligase. J. Biol. Chem. 280 (13), 13187–13194.

Ikeda, M., Yi, M., Li, K., Lemon, S.M., 2002. Selectable subgenomic and genome-length dicistronic RNAs derived from an infectious molecular clone of the HCV-N strain of hepatitis C virus replicate efficiently in cultured Huh7 cells. J. Virol. 76 (6), 2997–3006.

Kampmueller, K.M., Miller, D.J., 2005. The cellular chaperone heat shock protein 90 facilitates Flock House virus RNA replication in *Drosophila* cells. J. Virol. 79 (11), 6827–6837.

Kim, S.J., Kim, J.H., Kim, Y.G., Lim, H.S., Oh, J.W., 2004. Protein kinase C-related kinase 2 regulates hepatitis C virus RNA polymerase function by phosphorylation. J. Biol. Chem. 279 (48), 50031–50041.

Kukihara, H., Moriishi, K., Taguwa, S., Tani, H., Abe, T., Mori, Y., Suzuki, T., Fukuhara, T., Taketomi, A., Maehara, Y., Matsuura, Y., 2009. Human VAP-C negatively regulates hepatitis C virus propagation. J. Virol. 83 (16), 7959–7969.

Kyono, K., Miyashiro, M., Taguchi, I., 2002. Human eukaryotic initiation factor 4AII associates with hepatitis C virus NS5B protein in vitro. Biochem. Biophys. Res. Commun. 292 (3), 659–666.

Laporte, M.G., Jackson, R.W., Draper, T.L., Gaboury, J.A., Galie, K., Herbertz, T., Hussey, A.R., Rippin, S.R., Benetatos, C.A., Chunduru, S.K., Christensen, J.S., Coburn, G.A., Rizzo, C.J., Rhodes, G., O'Connell, J., Howe, A.Y., Mansour, T.S., Collett, M.S., Pevear, D.C., Young, D.C., Gao, T., Tyrrell, D.L., Kneteman, N.M., Burns, C.J., Condon, S.M., 2008. The discovery of pyrano [3, 4-b] indole-based allosteric inhibitors of HCV NS5B polymerase with in vivo activity. ChemMedChem 3 (10), 1508–1515.

Liu, H.M., Aizaki, H., Choi, K.S., Machida, K., Ou, J.J., Lai, M.M., 2009. SYNCRIP (synaptotagmin-binding, cytoplasmic RNA-interacting protein) is a host factor involved in hepatitis C virus RNA replication. Virology 386 (2), 249–256.

Lohmann, V., Körner, F., Herian, U., Bartenschlager, R., 1997. Biochemical properties of hepatitis C virus NS5B RNA-dependent RNA polymerase and identification of amino acid sequence motifs essential for enzymatic activity. J. Virol. 71 (11), 8416–8428.

Lohmann, V., Roos, A., Körner, F., Koch, J.O., Bartenschlager, R., 2000. Biochemical and structural analysis of the NS5B RNA-dependent RNA polymerase of the hepatitis C virus. J. Viral Hepat. 7 (3), 167–174.

Manns, M.P., Wedemeyer, H., Cornberg, M., 2006. Treating viral hepatitis C: efficacy, side effects, and complications. Gut 55 (9), 1350–1359.

Meyer, A.S., Gillespie, J.R., Walther, D., Millet, I.S., Doniach, S., Frydman, J., 2003. Closing the folding chamber of the eukaryotic chaperonin requires the transition state of ATP hydrolysis. Cell 113 (3), 369–381.

Momose, F., Naito, T., Yano, K., Sugimoto, S., Morikawa, Y., Nagata, K., 2002. Identification of Hsp90 as a stimulatory host factor involved in influenza virus RNA synthesis. J. Biol. Chem. 277 (47), 45306–45314.

Moradpour, D., Bieck, E., Hügle, T., Wels, W., Wu, J.Z., Hong, Z., Blum, H.E., Bartenschlager, R., 2002. Functional properties of a monoclonal antibody inhibiting the hepatitis C virus RNA-dependent RNA polymerase. J. Biol. Chem. 277 (1), 593–601.

Moriishi, K., Matsuura, Y., 2007. Host factors involved in the replication of hepatitis C virus. Rev. Med. Virol. 17 (5), 343–354.

Murakami, K., Ishii, K., Ishihara, Y., Yoshizaki, S., Tanaka, K., Gotoh, Y., Aizaki, H., Kohara, M., Yoshioka, H., Mori, Y., Manabe, N., Shoji, I., Sata, T., Bartenschlager, R., Matsuura, Y., Miyamura, T., Suzuki, T., 2006. Production of infectious hepatitis C virus particles in three-dimensional cultures of the cell line carrying the genome-length dicistronic viral RNA of genotype 1b. Virology 351 (2), 381–392.

Naito, T., Momose, F., Kawaguchi, A., Nagata, K., 2007. Involvement of Hsp90 in assembly and nuclear import of influenza virus RNA polymerase subunits. J. Virol. 81 (3), 1339–1349.

Nakagawa, S., Umehara, T., Matsuda, C., Kuge, S., Sudoh, M., Kohara, M., 2007. Hsp90 inhibitors suppress HCV replication in replicon cells and humanized liver mice. Biochem. Biophys. Res. Commun. 353 (4), 882–888.
Nelson, H.B., Tang, H., 2006. Effect of cell growth on hepatitis C virus (HCV) replication and a mechanism of cell confluence-based inhibition of HCV RNA and protein expression. J. Virol. 80 (3), 1181–1190.
Niwa, H., Yamamura, K., Miyazaki, J., 1991. Efficient selection for high-expression transfectants with a novel eukaryotic vector. Gene 108 (2), 193–199.
Okamoto, T., Nishimura, Y., Ichimura, T., Suzuki, K., Miyamura, T., Suzuki, T., Moriishi, K., Matsuura, Y., 2006. Hepatitis C virus RNA replication is regulated by FKBP8 and Hsp90. EMBO J. 25 (20), 5015–5025.
Okamoto, T., Omori, H., Kaname, Y., Abe, T., Nishimura, Y., Suzuki, T., Miyamura, T., Yoshimori, T., Moriishi, K., Matsuura, Y., 2008. A single-amino-acid mutation in hepatitis C virus NS5A disrupting FKBP8 interaction impairs viral replication. J. Virol. 82 (7), 3480–3489.
Parent, R., Qu, X., Petit, M.A., Beretta, L., 2009. The heat shock cognate protein 70 is associated with hepatitis C virus particles and modulates virus infectivity. Hepatology 49 (6), 1798–1809.
Pietschmann, T., Lohmann, V., Rutter, G., Kurpanek, K., Bartenschlager, R., 2001. Characterization of cell lines carrying self-replicating hepatitis C virus RNAs. J. Virol. 75 (3), 1252–1264.
Pietschmann, T., Lohmann, V., Kaul, A., Krieger, N., Rinck, G., Rutter, G., Strand, D., Bartenschlager, R., 2002. Persistent and transient replication of full-length hepatitis C virus genomes in cell culture. J. Virol. 76 (8), 4008–4021.
Saito, I., Miyamura, T., Ohbayashi, A., Harada, H., Katayama, T., Kikuchi, S., Watanabe, Y., Koi, S., Onji, M., Ohta, Y., Choo, Q.L., Houghton, M., Kuo, G., 1990. Hepatitis C virus infection is associated with the development of hepatocellular carcinoma. Proc. Natl Acad. Sci. USA 87 (17), 6547–6549.
Seeff, L.B., Hoofnagle, J.H., 2003. Appendix: the National Institutes of Health Consensus Development Conference: management of hepatitis C 2002. Clin. Liver Dis. 7 (1), 261–287.
Shi, S.T., Lee, K.J., Aizaki, H., Hwang, S.B., Lai, M.M., 2003. Hepatitis C virus RNA replication occurs on a detergent-resistant membrane that cofractionates with caveolin-2. J. Virol. 77 (7), 4160–4168.
Shimakami, T., Honda, M., Kusakawa, T., Murata, T., Shimotohno, K., Kaneko, S., Murakami, S., 2006. Effect of hepatitis C virus (HCV) NS5B-nucleolin interaction on HCV replication with HCV subgenomic replicon. J. Virol. 80 (7), 3332–3340.
Shirakura, M., Murakami, K., Ichimura, T., Suzuki, R., Shimoji, T., Fukuda, K., Abe, K., Sato, S., Fukasawa, M., Yamakawa, Y., Nishijima, M., Moriishi, K., Matsuura, Y., Wakita, T., Suzuki, T., Howley, P.M., Miyamura, T., Shoji, I., 2007. E6AP ubiquitin ligase mediates ubiquitylation and degradation of hepatitis C virus core protein. J. Virol. 81 (3), 1174–1185.
Suzuki, T., Ishii, K., Aizaki, H., Wakita, T., 2007. Hepatitis C viral life cycle. Adv. Drug Deliv. Rev. 59 (12), 1200–1212.
Taguwa, S., Okamoto, T., Abe, T., Mori, Y., Suzuki, T., Moriishi, K., Matsuura, Y., 2008. Human butyrate-induced transcript 1 interacts with hepatitis C virus NS5A and regulates viral replication. J. Virol. 82 (6), 2631–2641.
Taguwa, S., Kambara, H., Omori, H., Tani, H., Abe, T., Mori, Y., Suzuki, T., Yoshimori, T., Moriishi, K., Matsuura, Y., 2009. Cochaperone activity of human butyrate-induced transcript 1 facilitates hepatitis C virus replication through an Hsp90-dependent pathway. J. Virol. 83 (20), 10427–10436.
Tian, G., Vainberg, I.E., Tap, W.D., Lewis, S.A., Cowan, N.J., 1995. Specificity in chaperonin-mediated protein folding. Nature 375 (6528), 250–253.
Tu, H., Gao, L., Shi, S.T., Taylor, D.R., Yang, T., Mircheff, A.K., Wen, Y., Gorbalenya, A.E., Hwang, S.B., Lai, M.M., 1999. Hepatitis C virus RNA polymerase and NS5A complex with a SNARE-like protein. Virology 263 (1), 30–41.
Ujino, S., Yamaguchi, S., Shimotohno, K., Takaku, H., 2009. Heatshock protein 90 is essential for stabilization of the hepatitis C virus nonstructural protein NS3. J. Biol. Chem. 284 (11), 6841–6846.
Valpuesta, J.M., Martín-Benitoa, J., Gómez-Puertasa, P., Carrascosaa, J.L., Willison, K.R., 2002. Structure and function of a protein folding machine: the eukaryotic cytosolic chaperonin CCT. FEBS Lett. 529 (1), 11–16.
Wakita, T., Pietschmann, T., Kato, T., Date, T., Miyamoto, M., Zhao, Z., Murthy, K., Habermann, A., Krausslich, H.G., Mizokami, M., Bartenschlager, R., Liang, T.J., 2005. Production of infectious hepatitis C virus in tissue culture from a cloned viral genome. Nat. Med. 11 (7), 791–796.
Watashi, K., Ishii, N., Hijikata, M., Inoue, D., Murata, T., Miyanari, Y., Shimotohno, K., 2005. Cyclophilin B is a functional regulator of hepatitis C virus RNA polymerase. Mol. Cell 19 (1), 111–122.
Weng, L., Du, J., Zhou, J., Ding, J., Wakita, T., Kohara, M., Toyoda, T., 2009. Modification of hepatitis C virus 1b RNA polymerase to make a highly active JFH1-type polymerase by mutation of the thumb domain. Arch. Virol. 154 (5), 765–773.
Yaffe, M.B., Farr, G.W., Miklos, D., Horwich, A.L., Sternlicht, M.L., Sternlicht, H., 1992. TCP1 complex is a molecular chaperone in tubulin biogenesis. Nature 358 (6383), 245–248.
Yam, A.Y., Xia, Y., Lin, H.T., Burlingame, A., Gerstein, M., Frydman, J., 2008. Defining the TRiC/CCT interactome links chaperonin function to stabilization of newly made proteins with complex topologies. Nat. Struct. Mol. Biol. 15 (12), 1255–1262.
Yanagida, M., Miura, Y., Yagasaki, K., Taoka, M., Isobe, T., Takahashi, N., 2000. Matrix assisted laser desorption/ionization-time of flight-mass spectrometry analysis of proteins detected by anti-phosphotyrosine antibody on two-dimensional-gels of fibroblast cell lysates after tumor necrosis factor-alpha stimulation. Electorophoresis 21 (9), 1890–1898.
Yang, G., Pevear, D.C., Collett, M.S., Chunduru, S., Young, D.C., Benetatos, C., Jordan, R., 2004. Newly synthesized hepatitis C virus replicon RNA is protected from nuclease activity by a protease-sensitive factor(s). J. Virol. 78 (18), 10202–10205.

Biochemical and Biophysical Research Communications 417 (2012) 945–950

Contents lists available at SciVerse ScienceDirect

Biochemical and Biophysical Research Communications

journal homepage: www.elsevier.com/locate/ybbrc

Copy number of adenoviral vector genome transduced into target cells can be measured using quantitative PCR: Application to vector titration

Zheng Pei, Saki Kondo, Yumi Kanegae, Izumu Saito *

Laboratory of Molecular Genetics, Institute of Medical Science, University of Tokyo, 4-6-1 Shirokanedai, Minato-ku, Tokyo 108-8639, Japan

ARTICLE INFO

Article history:
Received 25 November 2011
Available online 19 December 2011

Keywords:
Adenovirus vector
Virus titer
Quantitative PCR

ABSTRACT

Both transfection and adenovirus vectors are commonly used in studies measuring gene expression. However, the real DNA copy number that is actually transduced into target cells cannot be measured using quantitative PCR because attached DNA present on the cell surface is difficult to distinguish from successfully transduced DNA. Here, we used Cre/*lox*P system to show that most of the transfected DNA was in fact attached to the cell surface; in contrast, most of the viral vector DNA used to infect the target cells was present inside the cells after the cells were washed according to the conventional infection protocol. We applied this characteristic to adenoviral vector titration. Current methods of vector titration using the growth of 293 cells are influenced by the effect of the expressed gene product as well as the cell conditions and culture techniques. The titration method proposed here indicates the copy numbers introduced to the target cells using a control vector that is infected in parallel (relative vector titer: rVT). Moreover, the new titration method is simple and reliable and may replace the current titration methods of viral vectors.

1. Introduction

Transfection is the most commonly used method of choice for examining the nature and function of a gene *in vivo* because this technique is very simple to perform and easy to manipulate. However, the copy numbers of DNA that successfully reach the inside of the target cells cannot be measured using quantitative PCR (qPCR), since experiments using qPCR cannot effectively distinguish DNA present inside the cells from DNA attached to and present on the cell surface. The first-generation adenovirus vector (FG AdV) is now commonly used for gene expression experiments, mainly because the resulting expression level is much higher than that achieved using transfection. Another reason is that the data offered by this vector is quantitative for a linearity range that is about 20-fold wider [1]. However, the vector system is also thought to be unsuitable for qPCR for the same reason mentioned above.

There are several methods for using FG AdV. The most popular titration methods are bioassays of plaque-forming unit (PFU) [2,3] and end-point cytopathic effect (CPE) assay or 50% tissue-culture infectious dose ($TCID_{50}$) assay [3,4]. These methods were actually developed for the titration of wild-type adenoviruses, and not for the titration of FG AdV. At least 4 days or up to 2 weeks are required to obtain the endpoint, and the results often vary depending on the conditions of the 293 cell lines, researchers and laboratories. The immunofluorescent focus assay using a florescent microscope [5,6] and the immunospot assay using 3,3′-diaminobenzidine staining [7] (TaKaRa Bio kit), count the foci of infected 293 cells expressing viral hexon protein. Although the titration can be completed in 2 days, these methods also rely on viral replication in 293 cells. The amount of AdV particles has been measured based on the optical density at 260 nm (OD_{260}) [8], although this method can only be used for purified virus stock. Because the AdVs replicate rapidly in growing 293 cells in all these methods, the titration results are sometimes influenced by the expressed product of an inserted gene if it disturbs viral replication or the growth of 293 cells. Consequently, sometimes the results do not reflect the actual copy number that was transferred to the target cells, which is undoubtedly the most important ability of a "vector".

qPCR has been used to calculate the copy numbers of AdV in viral stocks [9]. In the preparation of helper-dependent AdV (HD AdV), the contaminated helper virus (an FG AdV) in the viral stock has been measured using qPCR [10,11]. Another category of the qPCR method obtains the viral titer not by measuring AdV DNA in the viral stock, but by quantifying the copy numbers of *transduced viral genomes in the target cells* (genomic infectious titer,

Abbreviations: FG, first-generation; AdV, adenoviral vector; PFU, plaque-forming unit; $TCID_{50}$, 50% tissue-culture infectious dose; CPE, cytopathic effect; qPCR, quantitative real-time PCR; HD-AdV, helper-dependent AdV; GIT, genomic infectious titer; rVT, relative vector titer; MOI, multiplicity of infection; NLS, nuclear localization signal; OTC, Ornithine transcarbamylase.

* Corresponding author. Fax: +81 3 5449 5432.
E-mail address: isaito@ims.u-tokyo.ac.jp (I. Saito).

0006-291X/$ - see front matter © 2011 Elsevier Inc. All rights reserved.
doi:10.1016/j.bbrc.2011.12.016

GIT); the total DNA of the infected cells were extracted, and the viral DNA were detected using slot-blot hybridization [12] or qPCR [10,13]. Although all these methods are intended to measure the copy number of the viral genome, there are two problems with using them for the titration of FG AdV. One reason is similar to that described above for transfection but is more crucial: the obtained copy numbers include not only the viral genome of the internally transduced viral particles, but also the DNA of *non-infectious particles* and unpackaged naked DNA that is present either freely in the viral stock or attached to the surface of the target cells. The other problem is that the GIT fluctuates markedly depending on the target cell concentration and conditions; hence, GITs obtained at different times and places are difficult to compare. Therefore, both of these problems must be solved to establish a reliable GIT method. In this paper, we propose a new titration method that solves these problems.

2. Materials and methods

2.1. Cell lines and recombinant adenovirus

The human embryo kidney cell line 293 [14] constitutively expresses adenoviral E1 genes. The cell line CV-1 is derived from African green monkey kidney. HeLa cells are derived from human cervical cancer. The cell line NIH-3T3 was established from an NIH Swiss mouse embryo. AxCANCre, a Cre-expressing AdV tagged with a nuclear localization signal [15], and AxEFdsR, a dsRed-expressing AdV [16], have been described previously. The GFP-expressing AdV AxCAGFP was generated using the COS-TPC method [17]. The AdV AxEFLNLdsRed is identical to AxCALNLZ [15] except that the CAG promoter and the LacZ gene were replaced by the EF1α promoter, and the dsRed gene, respectively. The $TCID_{50}$ was measured according to the protocol described by Kanegae et al. [4]. The plasmid pA14cw contains the AdV genomic DNA of pAdex1w [17] from map units 0 to 14.

2.2. Southern blotting analysis

CV-1 cells in a 6-cm dish were infected with AxCANCre. After 24 h, the cells were infected with AxEFLNLdsRed or transfected with 1 μg of the plasmid pxEFLNLdsRed per 6-cm dish using Transfast (Promega). The total DNA was prepared from the dish [18]. Before alkaline treatment, the agarose gel was exposed to 0.1-N HCl for partial depurination causing DNA fragmentation to several hundred base pairs (bp) to obtain the complete transfer to the membrane [19]; the DNA was then transferred to the nylon membrane Hybond-N (Amersham GE) using the capillary-transfer method [20]. Specific DNA was detected using a DIGDNA Labeling and Detection Kit (Roche Diagnostics). The 0.6-kb *Xmn*I fragment derived from the EF1α promoter region was labeled with digoxigenin-UTP, and specific DNA was detected using the chemiluminescence of CDP-Star (Roche Diagnostics). The bands were visualized using LAS-4000 (Fuji Film) and the densitometry was performed using an image analysis program (Multi Gauge version 3X, Fuji Film). The linear correlation between the DNA amounts and the intensity of the bands was confirmed (Fig. S1 of Supplementary Data), showing that the Southern analysis was quantitative.

2.3. qPCR

The infected total cell DNA was prepared from cells, as described previously [18,21]. Alternatively, we confirmed the total cell DNA prepared using a DNA preparation kit (Macherey–Nagel through TaKaRa Bio). qPCR was performed to detect the AdV genome using a probe for the pIX gene [16] (Fig. 2A). The amount of chromosomal DNA was simultaneously measured to correct the Ct values of the viral genome per cell, and the corrected Ct was shown throughout. The probes were derived from the sequence of the human β-actin gene for HeLa, the human OTC gene for CV-1 [16], and the mouse GAPDH gene for NIH-3T3 (Applied Biosystems, catalog number 7000-1). The qPCR reaction was performed according to the manufacturer's protocol: 50 °C for 2 min and 95 °C for 10 min, followed by 40 cycles of 95 °C for 15 s and 60 °C for 1 min (Applied BioSystems).

2.4. Generation of a standard curve using qPCR

The copy numbers of the plasmid pA14cw containing the pIX sequences and the cosmid pAxcwit2 [22] containing the full-genome of the FG AdV [22] were calculated according to Puntel et al. [11]. The plasmid and cosmid were serially diluted (Fig. 2B and C). The equivalency between the molecular weight of the plasmid pA14cw and the number of copies was calculated by considering the pA14cw molecular weight and the equivalency between base pairs (pA14cw [4,247 bp]) and Daltons (Da) ($1bp_{Ad5}$ = 678 Da). $Mass_{pA14cw}$ (Da) = 4,247 bp/molecule × 678 Da/bp = 2.88×10^6 Da/molecule. We obtained the equivalency of mass 2.88×10^6 Da/molecule × 1.66×10^{-18} μg/Da = 4.78×10^{-12} μg/molecule. The copy numbers of the cosmid pAxcwit2 (42, 698 bp) were similarly calculated.

3. Results and discussion

3.1. Quantification of internally transduced viral copies in target cells

To establish a reliable GIT method, determining the ratio of successfully internalized viral DNA to DNA that has physically attached to the cell surface (that is, naked viral DNA or DNA in inactivated viral particles in AdV-infected target cells) is essential. To estimate the amounts of the former and the latter, we utilized the Cre/*lox*P system. CV-1 cells were infected with the AdV AxCANCre expressing Cre at an MOI of 5. Then, 24 h later, the cells were infected with the target AdV AxEFLNLdsRed at an MOI of 7.5 or were transfected with 1 μg of the target plasmid pxEFLNLdsRed as a control. The target unit in the AdV and the plasmid contains the same sequences of the EF1α promoter and the dsRed gene flanked by two *lox*Ps (Fig. 1A). The total cell DNA was extracted after the indicated number of days and digested with *Bgl*II; the DNA of the target unit was detected using a Southern technique (Fig. 1B and C). The 2.8-kb band (S2.8) indicates the substrate originally present before Cre-mediated recombination, i.e., the unprocessed substrate, while the 1.5-kb band (R1.5) shows the presence of the recombined product. We considered that the viral DNA and the transfected DNA that are physically attached to the cell surface cannot be processed by Cre and remain as unprocessed substrate.

When the cells were transfected with the target plasmid, the majority of the target DNA remained unprocessed even after 72 h (Fig. 1C, column 6). A densitometry analysis showed that only 9 ± 2% (n = 7) of the DNA was processed substrate. Also, a preliminary experiment showed that when using 3 μg of plasmid DNA, the percentage was 12% (data not shown). These results suggested that most of the transfected DNA was possibly present on the cell surface and that the DNA copy number after transfection did not reflect that of the internalized DNA molecules. In contrast, most of the target viral DNA was processed using Cre-mediated recombination by 2 or 3 days after infection (Fig. 1B, columns 5 and 6); the recombination efficiency was 92 ± 3% (n = 4). Considering that the recombination efficiency must not be 100%, the result suggested that at least 92% of the target viral DNA was present inside the infected cells. Similar results were obtained when using

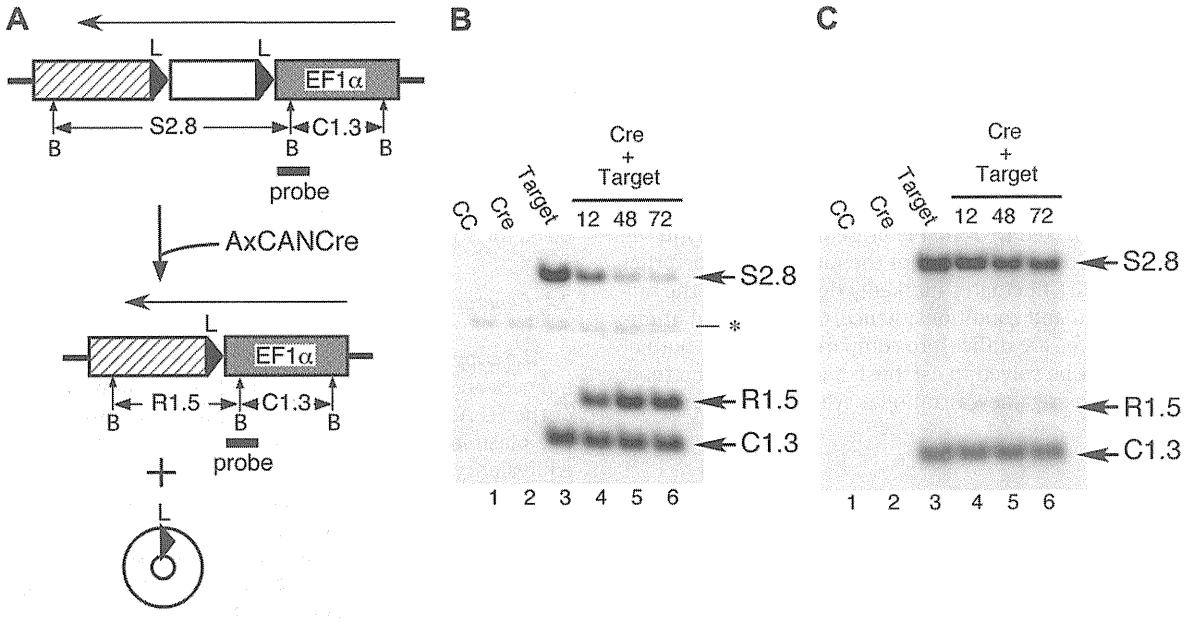

Fig. 1. (A) Structure of the target unit of recipient virus and plasmid. White box, stuffer DNA consisting of neo gene plus polyadenylation (poly(A)) sequence; shadowed box, cDNA plus poly(A) sequence; solid triangle, *lox*P sequence. Arrows show the direction of transcription. (B) Cre-mediated recombination using AdV. CC, uninfected; Cre, AxCANCre; Target, AxEFLNLdsRed. The numbers show the hours after infection. The asterisk shows the sequence of the EF1α gene in the human chromosome. (C) Cre-mediated recombination using plasmid transfection. The representations are the same in (B). For the densitometry four and seven independent experiments in (B) and (C) were performed, respectively.

different MOIs from 1 to 10 (Fig. S2). Therefore, the result showed that nearly all the detected viral DNA was derived from internalized, actively infectious viral particles; hence, the quantification of viral genomes using qPCR can be reliably used for titration.

3.2. Measurement of AdV-genome copies in infected cells using qPCR

A set of TaqMan PCR primers and probes were designed for detecting the AdV genome in the viral pIX coding region, since this gene is present closest to the target insert and encodes a viral structural protein that is essential for stable viral particles (Fig. 2A). The method for quantifying the copy number of FG AdV DNA in infected cells was essentially that described by Ma et al. [9]. The sensitivity of detection and the linear range of the quantification of this qPCR were determined by serial dilution of the 4.2-kb plasmid pA14cw containing the pIX gene and the 42.7-kb cosmid pAxcwit2 containing the full-length genome of the AdV backbone (Fig. 2B and C). The linear range for quantification was found to be between at least 10^3 and 10^9 copies for the plasmid template pA14cw per 5 μL; a plot of the plasmid copy number versus the Ct value between 7 and 27 was linear on a logarithmic scale with a coefficient correlation (r^2) of 0.99 (Fig. 2B). The cosmid template Axcwit2 produced an identical result (Fig. 2C), confirming that the Ct value accurately depended on the copy numbers irrespective of the DNA size. Based on these results, the Ct values obtained using our PCR system can be converted to the copy numbers for a given DNA sample.

As the next step in the titration using qPCR, CV-1 cells in the well of a 24-well plate (2.0×10^5 cells) were infected using the suspension method (see below) with 10 μL of serially diluted stocks of AxCAGFP virus ("control virus stock" for the conversion of the viral Ct value to the copy number *when using our particular qPCR machine*), and the total infected cell DNA was extracted and the Ct values of the viral genome corrected using the Ct value of the cell DNA (see Section 2) were measured (Fig. 2D). A linear correlation of the Ct values to the dilutions was observed from 18 to at least 28. Therefore, together with the results shown in Fig. 2C, the GIT, i.e., the copy number of the transduced viral genome per cell for this cell concentration of 2.0×10^5 cells, can be calculated. For example, a 10^{-2} dilution of 10 μL of viral stock produced a Ct value of 24.34 according to the equation shown in Fig. 2D ($y = 2.97x + 18.4$), and the same Ct value using that shown in Fig. 2C ($y = 24.34 = -3.4x + 38.2$) corresponded to $10^{4.08} \approx 1.2 \times 10^4$ copies of viral genome in 5 μL, i.e., *the GIT titer of the control virus stock was* 2.4×10^8 *copies/mL* ($1.2 \times 10^4 \times 10^3/5 \times 1/10^{-2}$). As described above, because the equations for the plasmid (Fig. 2B) and the cosmid (Fig. 2C) were practically identical, not the cosmid but a plasmid containing the pIX gene can be used for the conversion of the vital Ct value to the copy number. This method of obtaining the GIT of a control virus is essential for rVT because the Ct value differs depending on the qPCR machine. If the $TCID_{50}$ titer of this control virus is known, the $TCID_{50}$ titer can be converted to the copy number/mL (see Section 3.5).

3.3. Establishment of the method for relative vector titer (rVT)

To examine the effect of the cell concentration on the GIT, HeLa cells at densities of 0.6, 2.0 and 6.0×10^5 (full sheet condition) per 6-well plate were infected in parallel with a virus of unknown titer (testing virus) and the virus AxCAGFP (control virus, the same virus used in Fig. 2D). Three days later, the total cell DNA was extracted. For each DNA sample, the Ct values of not only the viral DNA but also the cell chromosome DNA were simultaneously measured to correct for fluctuations in the cell numbers (see Section 2). The transduced copy numbers/mL, i.e. the GIT, vary markedly from 1 to 3.2 and 4.9 in their ratio as reported by Sandig et al. [13] (columns "GIT ratio", lines "HeLa"). This is the second reason why the GIT method cannot be directly used as a titration method. Similar result was obtained when using CV-1 cells (data not shown). In addition to human HeLa cells, monkey CV-1 cells and mouse NIH-3T3 cells were infected with the testing and control viruses and GITs, i.e., the transduced number of copies, were measured (lines "HeLa 6.0", "CV-1 6.0" and "NIH-3T3 6.0"). While the GITs of CV-1 and NIH-3T3 cells were 3-fold and 17-fold lower than that

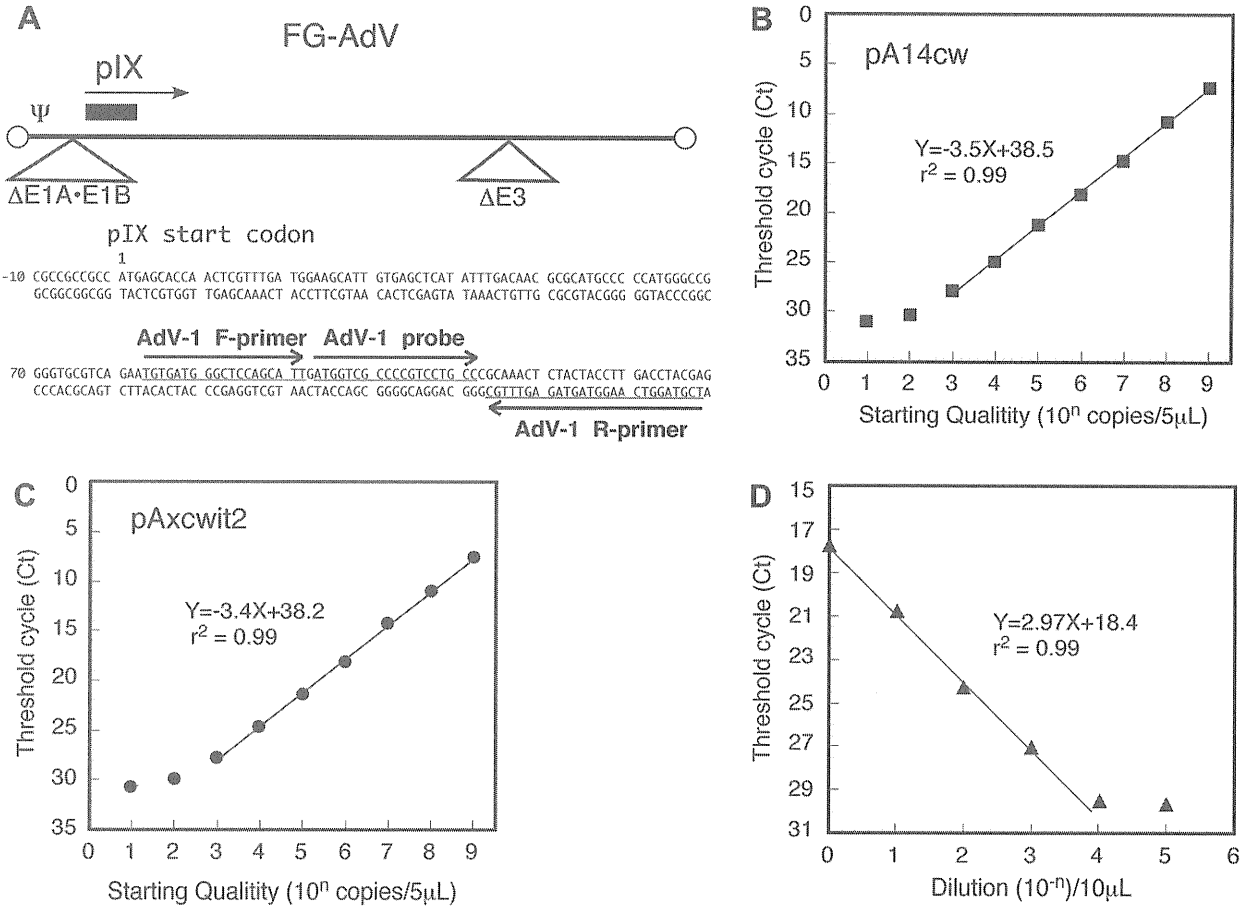

Fig. 2. (A) Position of the AdV-1 primers and the fluorogenic probe. The locations of the packaging signal (Ψ) and the coding region of the pIX gene are indicated. The arrows indicate the direction of transcription. AdV-1 F-primer, R-primer, and probe were designed using the program Primer Express 1.5 (Applied Biosystems), and their sequences are underlined. The primers and probes were selected according to the manufacturer's guidelines. The fluorogenic probes contained FAM (6-carboxylfluoroescein) at the 5′-end and TAMRA (6-carboxyltetramethylrhodamine) at the 3′-end. This set of primers/probe recognizes the coding region of the pIX gene. (B), (C), and (D) are the standard calibration curves for plasmids, cosmids and FG-AdV including the pIX gene, respectively. The standard calibration curves for the threshold cycle values (Ct) versus the copy number using serial dilutions of pA14cw (B) or pAxcwit2 (C) are shown. Similarly, serial dilutions of AxCAGFP vectors were used to generate the standard curve (D). The coefficients of correlation (r^2) are indicated.

of HeLa cells, respectively (column "GIT ratio", 0.3 for CV-1 and 0.06 for NIH-3T3), showing that GIT varied among different cell types.

However, because the control virus infected in parallel was identically influenced by the infection conditions, including the cell concentration and the cell type, the copy numbers of testing virus relative to that of the control virus can be calculated using the Ct value of the control virus as shown below. The relative GIT, called the rVT, is defined as follows:

$$\text{rVT} = (\text{control virus GIT}) \times 2^{(\text{control viral Ct}-\text{testing viral Ct})}(/\text{mL})$$

(Note that, because one *lower* Ct value means 2-fold *more* DNA, "$2^{(\text{testing viral Ct}-\text{control viral Ct})}$" is not correct).

For example, if control virus GIT, control viral Ct and testing viral Ct are 2.4×10^8 (copies/mL), 22.6 and 19.4, respectively, in a particular titration using CV-1 cells, the $\text{rVT} = 2.4 \times 10^8 \times 2^{(22.6-19.4)} = 2.4 \times 10^8 \times 2^{3.2} = 2.2 \times 10^9$ (copies/mL).

Because the rVTs of CV-1 and HeLa cells at the concentrations of 6.0×10^5 cells per well (full-sheet condition) were similar, i.e., 2.3×10^9 (copies/mL), the rVT calculated using the data of Fig. 2D can be applied to the rVT of HeLa cells. The rVTs measured using HeLa cell concentrations of 0.6×10^5, 2.0×10^5 and 6.0×10^5 cells per well were 0.9×10^9, 1.0×10^9 and 2.3×10^9 copies/μL, respectively (Table 1, rVT/mL): the ratio of rVTs obtained using three different cell concentrations (column "rVT ratio") was 0.4:0.4:1. Similar experiments using CV-1 cells indicated that the ratio was 1.2:1.2:1, showing that the rVT was less influenced by the cell concentration than the GIT. Table 1 also showed that, though the GIT of NIH-3T3 was extremely different from that of HeLa and CV-1, the rVT of NIH-3T3 was very similar to those of CV-1 and HeLa (column of "rVT ratio"). Therefore, even using different cell lines and dilutions, the rVT did not fluctuate, indicating that about the same rVT can be obtained using various types of cells other than HeLa cells for the purpose of titration. Because HeLa cells are commonly used worldwide, we recommend the use of HeLa cells for rVT measurements. Importantly, the present results also showed that the

Table 1
Differences between GIT and rVT among various cell concentration and cell lines.

Cells	No. of cells $\times 10^5$	GIT Copies/mL $\times 10^9$	GIT Ratio	rVT rVT/mL $\times 10^9$	rVT Ratio
HeLa	0.6	137.8 ± 6.4	4.9	0.9 ± 0.4	0.4
	2.0	89.5 ± 2.0	3.2	1.0 ± 0.2	0.4
	6.0	28.2 ± 1.8	1	2.3 ± 0.1	1
CV-1	6.0	8.2 ± 1.7	0.3	2.3 ± 0.1	1.0
NIH3T3 6.0	6.0	1.7 ± 0.3	0.06	1.0 ± 0.4	0.4

Two independent experiments were performed using the virus dilutions of 10^1 and 10^2.

Table 2
Infection conditions.

Condition	GIT/mL ($\times 10^9$)	Ratio
Plate	0.8 ± 0.3	1
Suspension	0.8 ± 0.2	1.0

The presentations are the same as Table 1.

Table 3
Days after infections.

Day	GIT/mL ($\times 10^9$)	Ratio
1	2.5 ± 0.1	1.6
2	1.6 ± 0.1	1
3	1.6 ± 0.4	1.0

The presentations are the same as Table 1.

rVT can be compared even when different cell lines or amounts of AdV were used.

The quality of the control virus does not significantly influence on the rVT value as far as the same lot of the control virus is used. Therefore, a conventional virus can be used as the control virus without purification. If strict comparison between the rVTs measured in different laboratories is needed, the adenovirus type 5 reference material may be useful and is available from ATCC (VR-1516) [23]. If a gene product of the testing virus is extremely deleterious to the target cells, the infected cells possibly grow slowly and the ratio of the copy number of the viral genome against that of β-actin on the cell chromosome may increase. However, if this is the case, the obtained rVT values of 10^{-1} dilution (high dose) and 10^{-2} dilution (low dose) must differ significantly, because the latter should be less influenced than the former. We have not experienced these cases.

3.4. Examination of infection conditions

We also examined whether the transduction efficiency of AdV differs when the cells to be infected are attached to a plate (plating method) or present in suspension (suspension method). In the former method, a monolayer of cells on the plate was incubated with an aliquot of AxCAGFP stock for 1 h for 37 °C, with shaking every 15 min before adding the medium. In the latter method, cells detached by trypsin were mixed with the virus, incubated for 5 min at room temperature, mixed with medium, and transferred to a 6-well or 24-well plate. The results showed no significant differences between the two methods for two different virus dilutions (Table 2). Because the suspension method is very simple and quick, we used the suspension method thereafter. Next, we examined the detected copy numbers of the transduced viral genome on days 1, 2 and 3. After washing the cells with PBS (−) on each day, the total infected-cell DNA was extracted, and the amounts of AdV genome were measured using qPCR (Table 3). The detected AdV copy number on day 1 was higher than that on day 2, but those on day 2 and day 3 were equal, suggesting that the number had reached a plateau level. The results were consistent with those for the Southern blot experiments (Fig. 1B, 48 h and 72 h). Consequently, we adopted day 2 for the measurement of rVT. Therefore, for the rVT method the infection protocol is very simple, and titration results can be obtained in only 2 days. The use of the infection protocol is not limited to AdV titration, but can also be used for ordinary AdV infection experiments. The rVT protocol is described in Supplementary Information.

3.5. Examples where the $TCID_{50}$ titer differed from the rVT

The ratio of the rVT value and the authentic $TCID_{50}$ titer were well correlated. AxEFLNLG is one example of an FG AdV; this AdV expresses neo protein unless the neo gene flanked by a pair of *lox*Ps is excised during Cre-mediated recombination. Because the neo gene is popularly used to establish neo-resistant cell lines, it must not be toxic. The rVT/mL and $TCID_{50}$/mL of a viral stock of this AdV were measured using CV-1 cells as a target and 293 cells, in which AdV proliferates, respectively. As shown in Table 4, in the first line, the ratio of rVT/$TCID_{50}$ was 0.3 using CV-1 for rVT; if HeLa cells are used for the rVT, the ratio should be $0.3 \times 0.6 \approx 0.2$ based on the data in Table 1. Thus, the $TCID_{50}$/mL was normally five times higher than the rVT/mL value when using HeLa as the target cells. Therefore, the ratio is normally useful when converting the values from one to another.

Table 4
Differences between rVT and $TCID_{50}$.

AdVs	rVT/mL	$TCID_{50}$/mL	rVT/$TCID_{50}$	Ratio
AxEFLNLG	$0.4 \pm 0.1 \times 10^9$	$1.8 \pm 0.2 \pm 10^9$	0.2	1
AxEFdsRed	$2.3 \pm 0.1 \times 10^9$	$0.3 \pm 0.1 \pm 10^9$	7.7	34.5
AxCANCre	$2.6 \pm 0.4 \times 10^7$	$3.1 \pm 0.9 \pm 10^7$	0.8	3.8

The presentations are the same as Table 1.

However, the ratio sometimes differed; for AxEFdsRed, an AdV that highly expresses dsRed protein, the copy number transduced to the target cells obtained using rVT was 18-times higher than that obtained using the $TCID_{50}$ method. AxCANCre, which highly expresses Cre recombinase, also produced an rVT value that was 3.3-times higher than that obtained using the $TCID_{50}$ method. Because the rVT value reflects the copy numbers in transduced target cells that are important for expression experiments, it is more valuable than the $TCID_{50}$ titer. Also, the rVT method can be applied for the titration of viruses that cannot proliferate in 293 cells, such as HD-AdV and other DNA and RNA viral vectors that do not replicate in the target cells.

In summary, we used Cre recombination and showed that the majority of the AdV genome detected in infected cells indicated successfully transduced molecules and that qPCR can certainly be used for AdV titration. Although cell concentrations and cell types influence the GIT tremendously, these factors can be corrected using a "control AdV" in parallel; hence, we established the rVT method, which can be used to determine the amount of actively infectious AdV genome present in the target cells. This method is quick, reliable, and superior to current titration methods using 293 cells.

Acknowledgments

The authors thank Ms. M. Terashima and Mr. Y. Ohno for technical support. Funding for this research was provided by a Grant in Aid for Scientific Research on Priority Areas from Ministry of Education, Culture, Sports, Science and Technology, Japan (to I.S.).

Appendix A. Supplementary data

Supplementary data associated with this article can be found, in the online version, at doi:10.1016/j.bbrc.2011.12.016.

References

[1] S. Kondo, Y. Takata, M. Nakano, I. Saito, Y. Kanegae, Activities of various FLP recombinases expressed by adenovirus vectors in mammalian cells, J. Mol. Biol. 390 (2009) 221–230.

[2] F.L. Graham, A.J. van der Eb, A new technique for the assay of infectivity of human adenovirus 5 DNA, Virology 52 (1973) 456–467.

[3] B. Precious, W.C. Russell, Growth, purification and titration of adenovirus, in: B.M. Mahy (Ed.), Virology: A Practical Approach, IRL Press, Oxford, 1985, pp. 193–205.
[4] Y. Kanegae, M. Makimura, I. Saito, A simple and efficient method for purification of infectious recombinant adenovirus, Jpn. J. Med. Sci. Biol. 47 (1994) 157–166.
[5] R. Mentel, E. Matthes, M. Janta-Lipinski, U. Wegner, Fluorescent focus reduction assay for the screening of antiadenoviral agents, J. Virol. Methods 59 (1996) 99–104.
[6] L. Philipson, Adenovirus assay by the fluorescent cell-counting procedure, Virology 15 (1961) 263–268.
[7] B. Bewig, W.E. Schmidt, Accelerated titering of adenoviruses, Biotechniques 28 (2000) 870–873.
[8] N. Mittereder, K.L. March, B.C. Trapnell, Evaluation of the concentration and bioactivity of adenovirus vectors for gene therapy, J. Virol. 70 (1996) 7498–7509.
[9] L. Ma, H.A. Bluyssen, M. De Raeymaeker, V. Laurysens, N. van der Beek, H. Pavliska, A.J. van Zonneveld, P. Tomme, H.H. van Es, Rapid determination of adenoviral vector titers by quantitative real-time PCR, J. Virol. Methods 93 (2001) 181–188.
[10] J. Crettaz, C. Olague, A. Vales, I. Aurrekoetxea, P. Berraondo, I. Otano, S. Kochanek, J. Prieto, G. Gonzalez-Aseguinolaza, Characterization of high-capacity adenovirus production by the quantitative real-time polymerase chain reaction: a comparative study of different titration methods, J. Gene Med. 10 (2008) 1092–1101.
[11] M. Puntel, J.F. Curtin, J.M. Zirger, A.K. Muhammad, W. Xiong, C. Liu, J. Hu, K.M. Kroeger, P. Czer, S. Sciascia, S. Mondkar, P.R. Lowenstein, M.G. Castro, Quantification of high-capacity helper-dependent adenoviral vector genomes in vitro and in vivo, using quantitative TaqMan real-time polymerase chain reaction, Hum. Gene Ther. 17 (2006) 531–544.
[12] F. Kreppel, V. Biermann, S. Kochanek, G. Schiedner, A DNA-based method to assay total and infectious particle contents and helper virus contamination in high-capacity adenoviral vector preparations, Hum. Gene Ther. 13 (2002) 1151–1156.
[13] V. Sandig, R. Youil, A.J. Bett, L.L. Franlin, M. Oshima, D. Maione, F. Wang, M.L. Metzker, R. Savino, C.T. Caskey, Optimization of the helper-dependent adenovirus system for production and potency in vivo, Proc. Natl. Acad. Sci. USA 97 (2000) 1002–1007.
[14] F.L. Graham, J. Smiley, W.C. Russell, R. Nairn, Characteristics of a human cell line transformed by DNA from human adenovirus type 5, J. Gen. Virol. 36 (1977) 59–74.
[15] Y. Kanegae, G. Lee, Y. Sato, M. Tanaka, M. Nakai, T. Sakaki, S. Sugano, I. Saito, Efficient gene activation in mammalian cells by using recombinant adenovirus expressing site-specific Cre recombinase, Nucleic Acids Res. 23 (1995) 3816–3821.
[16] Y. Kanegae, M. Terashima, S. Kondo, H. Fukuda, A. Maekawa, Z. Pei, I. Saito, High-level expression by tissue/cancer-specific promoter with strict specificity using a single-adenoviral vector, Nucleic Acids Res. 39 (2010) e7.
[17] S. Miyake, M. Makimura, Y. Kanegae, S. Harada, Y. Sato, K. Takamori, C. Tokuda, I. Saito, Efficient generation of recombinant adenoviruses using adenovirus DNA-terminal protein complex and a cosmid bearing the full-length virus genome, Proc. Natl. Acad. Sci. USA 93 (1996) 1320–1324.
[18] I. Saito, Y. Oya, K. Yamamoto, T. Yuasa, H. Shimojo, Construction of nondefective adenovirus type 5 bearing a 2.8-kilobase hepatitis B virus DNA near the right end of its genome, J. Virol. 54 (1985) 711–719.
[19] I. Saito, R. Groves, E. Giulotto, M. Rolfe, G.R. Stark, Evolution and stability of chromosomal DNA coamplified with the CAD gene, Mol. Cell Biol. 9 (1989) 2445–2452.
[20] J. Sambrook, D.W. Russell, Molecular Cloning, third ed., Cold Spring Harbor Laboratory Press, New York, 2001.
[21] M. Nakano, K. Odaka, Y. Takahashi, M. Ishimura, I. Saito, Y. Kanegae, Production of viral vectors using recombinase-mediated cassette exchange, Nucleic Acids Res. 33 (2005) e76.
[22] H. Fukuda, M. Terashima, M. Koshikawa, Y. Kanegae, I. Saito, Possible mechanism of adenovirus generation from a cloned viral genome tagged with nucleotides at its ends, Microbiol. Immunol. 50 (2006) 643–654.
[23] B. Huchins, N. Sajjadi, S. Seaver, A. Shepherd, S.R. Bauer, S. Simek, K. Carson, E. Aguilar-Cordova, Working toward an adenoviral vector testing standard, Mol. Ther. 2 (2000) 532–534.

Virus Research 160 (2011) 89–97

Contents lists available at ScienceDirect

Virus Research

journal homepage: www.elsevier.com/locate/virusres

Conditional gene expression in hepatitis C virus transgenic mice without induction of severe liver injury using a non-inflammatory Cre-expressing adenovirus

Tomoko Chiyo[a], Satoshi Sekiguchi[a], Masahiro Hayashi[a], Yoshimi Tobita[a], Yumi Kanegae[b], Izumu Saito[b], Michinori Kohara[a,*]

[a] Department of Microbiology and Cell Biology, The Tokyo Metropolitan Institute of Medical Science, 1-6, Kamikitazawa 2-chome, Setagaya-ku, Tokyo 156-8505, Japan
[b] Laboratory of Molecular Genetics, Institute of Medical Science, The University of Tokyo, Tokyo 108-8639, Japan

ARTICLE INFO

Article history:
Received 29 December 2010
Received in revised form 19 May 2011
Accepted 20 May 2011
Available online 30 May 2011

Keywords:
HCV transgenic mouse
Cre/loxP system
Recombinant adenovirus vector
EF1α promoter
Hepatitis

ABSTRACT

We previously established inducible-hepatitis C virus (HCV) transgenic mice, which expressed the HCV gene (nucleotides 294–3435) encoding the core, E1, E2, and NS2 proteins. The expression of these proteins is regulated by the Cre/loxP system and an adenovirus vector (AdV) that expresses Cre DNA recombinase (Cre) controlled by the CAG promoter (AxCANCre). Recent studies have demonstrated that AxCANCre injection alone results in severe liver injury by induction of the adenovirus protein IX (Ad-pIX) gene. As a result, HCV protein expression in transgenic mice livers was only short-term. In contrast, the EF1α promoter-bearing AdV induces slight Ad-pIX gene expression without inducing severe liver injury. Therefore, in the present study, we developed a Cre-expressing AdV that bears the EF1α promoter (AxEFCre) to express HCV protein in the transgenic mouse livers. In the non-transgenic mice injected with AxCANCre, alanine aminotransferase (ALT) levels were elevated and severe liver inflammation occurred; this was not observed in AxEFCre-injected mice. In contrast, AxEFCre-injected HCV transgenic mice showed milder liver inflammatory responses that were clearly due to HCV protein expression. Moreover, the AxEFCre injection enabled the transgenic mice to persistently express HCV protein. These results indicate that use of AxEFCre efficiently promotes Cre-mediated DNA recombination *in vivo* without a severe hepatitis response to AdV. This inducible-HCV transgenic mouse model using AxEFCre should be useful for research on HCV pathogenesis.

1. Introduction

Infection with the hepatitis C virus (HCV) is a major global health problem, as persistent viral infection leads to liver cirrhosis and hepatocellular carcinoma (Goodman and Ishak, 1995; Shepard et al., 2005). The chimpanzee is the only validated animal model for *in vivo* studies of HCV infection, while *in vivo* studies on the pathogenesis of HCV have been conducted using new animal models (Kremsdorf and Brezillon, 2007). Several groups have established transgenic mice that constitutively express single or multiple HCV protein(s) in the liver (Lerat et al., 2002; Moriya et al., 1997). However, in these mice, HCV protein expression begins *in utero*; as a result, they develop immune tolerance to the HCV antigens, and HCV-specific cellular responses or liver inflammation cannot be induced. To overcome these obstacles, we previously developed immunocompetent HCV transgenic mice in which HCV protein expression was tightly regulated by the Cre/*lox*P system (Wakita et al., 1998).

The E1- and E3-deleted adenovirus vector (AdV) has been widely used for both basic studies of gene function and for gene therapy *in vivo*. To deliver the *Cre* gene into the livers of HCV transgenic mice, we used an AdV that carries the CAG promoter linked to a nuclear localization signal-tagged Cre (AxCANCre), which has been used for Cre-mediated DNA recombination (Baba et al., 2005; Kobayashi et al., 2000; Shintani et al., 1999; Wakita et al., 1998). While AdV is relatively efficient in inducing transgene expression, several studies have shown that the viral vector itself can induce strong inflammatory responses in murine livers (Kafri et al., 1998; Wakita et al., 2000). Moreover, expression of transgenes via AdVs persists for only 2–4 weeks due to elimination of infected cells through immune responses directed against the AdVs (Akagi et al., 1997; Bangari and Mittal, 2006; Kafri et al., 1998; Sun et al., 2005; Wakita et al., 2000). To address these problems, the viral

* Corresponding author. Tel.: +81 3 5316 3232; fax: +81 3 5316 3137.
E-mail addresses: chiyo-tm@ncnp.go.jp (T. Chiyo), sekiguchi-st@igakuken.or.jp (S. Sekiguchi), mahayashi-kyt@umin.ac.jp (M. Hayashi), tobita-ys@igakuken.or.jp (Y. Tobita), kanegae@ims.u-tokyo.ac.jp (Y. Kanegae), isaito@ims.u-tokyo.ac.jp (I. Saito), kohara-mc@igakuken.or.jp (M. Kohara).

0168-1702/$ – see front matter © 2011 Elsevier B.V. All rights reserved.
doi:10.1016/j.virusres.2011.05.019

genes that cause cellular immune responses have been investigated. Recently, Nakai et al. (2007) reported that co-expression of adenovirus protein IX (Ad-pIX) resulted in AdV-induced immune responses. However, AdVs that carried the EF1α promoter did not induce Ad-pIX or increase the alanine aminotransferase (ALT) level, facilitating long-term transgene expression in mice.

In the present study, we generated a Cre-expressing AdV bearing the EF1α promoter (AxEFCre) to enable the persistent expression of HCV protein in the livers of inducible-HCV transgenic mice regulated by the Cre/*lox*P recombination system. When this AdV was used to express Cre in the HCV transgenic mouse livers, it induced less severe inflammatory responses and improved the long-term expression of HCV proteins compared to CAG promoter-bearing AdVs. Thus, AxEFCre efficiently promotes Cre-mediated DNA recombination *in vivo* without a severe hepatitis response to AdV and should be useful for HCV gene expression in the HCV transgenic mice.

2. Materials and methods

2.1. Cells

The 293 cells [CRL-1573, a human embryonic kidney cell line that contains the Ad5 E1 region; American Type Culture Collection (ATCC)] and HepG2 cells (HB-8065, a human hepatocellular carcinoma cell line; ATCC) were maintained in Dulbecco's modified Eagle's medium (DMEM; Nissui Pharmaceutical) supplemented with 10% fetal bovine serum (FBS; JRH Biosciences), 100 U/mL penicillin, and 100 μg/mL streptomycin (GIBCO) (10% FBS-DMEM). In addition, HepG2 cells containing the Cre reporter unit CALNLZ (Baba et al., 2005), termed Hep-CALNLZ cells, were selected for resistance to G418 (300 μg/mL; Sigma) and cultured in 10% FBS-DMEM.

2.2. Adenovirus vectors

E1- and E3-deleted AdVs derived from human adenovirus type 5 encoding expression units with a leftward orientation were used in this study. As expression units, untagged Cre or NLS-tagged Cre under the control of the CAG promoter (AxCANCre or AxCACre), untagged Cre or NLS-tagged Cre under the control of the EF1α promoter (AxEFNCre or AxEFCre), and untagged β-galactosidase (LacZ) under the control of the EF1α promoter (AxEFLacZ) were constructed (Fig. 1A). AxCANCre and AxCACre were generated as described previously (Kanegae et al., 1995). AxEFNCre, AxEFCre, and AxEFLacZ were constructed using pAxEFwtit2 DNA/RE Treatment (Nippon Gene). All of the AdVs were purified using two rounds of CsCl gradient centrifugation, and the titers of the concentrated and purified virus stocks were determined as described previously (Kanegae et al., 1994).

2.3. Animal procedures

HCV transgenic mice CN2-29 (C57BL/6 background) and normal C57BL/6 mice were used in the experiments. The CN2-29 transgenic mice express HCV genotype 1b proteins (core, E1, E2, and NS2 proteins) under the regulation of the Cre/*lox*P conditional switching system (Wakita et al., 1998). The transgenic mice were intravenously injected with each AdV at a dose of 1.0×10^9 plaque-forming units (PFU), and sacrificed 0.5, 7, or 21 days after injection for liver histology and biochemical analysis. All mice were bred in a pathogen-free facility and tested routinely for mouse hepatitis virus and other pathogens. All experiments using mice were approved by The Tokyo Metropolitan Institute of Medical Science Animal Experiment Committee and were performed in accordance with the animal experimentation guidelines of The Tokyo Metropolitan Institute of Medical Science.

2.4. Western blot detection of Cre and Ad-pIX

The HepG2 cells were placed in collagen-coated, 12-well plates and infected with the AdVs at a multiplicity of infection (MOI) of 20 or 100 for Western blot detection of Cre or Ad-pIX, respectively. After 24 h, the cells were washed with phosphate-buffered saline (PBS) and resolved in radioimmunoprecipitation assay (RIPA) buffer [10 mM Tris–HCl (pH 7.5), 0.15 M NaCl, 1% sodium dodecyl sulfate (SDS), 0.5% Nonidet P-40, protease inhibitor cocktail (Complete; Roche Molecular Biochemicals)]. The protein concentrations of the cell lysates were measured using the DC protein assay (Bio-Rad Laboratories). The cell lysates were electrophoresed on SDS–polyacrylamide gel, transferred to polyvinylidene difluoride membrane (GE Healthcare) activated with methanol, and blocked with 5% skim milk in PBS containing 0.1% Tween-20 (PBST). After washing with PBST, the membrane was incubated overnight at 4 °C in the presence of anti-Cre rabbit polyclonal antibody or anti-Ad-pIX rabbit polyclonal antibody (Nakai et al., 2007) prepared from hyper-immune rabbit sera, or anti-β-actin mouse monoclonal antibody (Sigma), followed by incubation with horseradish peroxidase (HRP)-conjugated $F(ab')_2$ of anti-rabbit or mouse IgG (GE Healthcare) for 1 h at room temperature. The expression levels of these proteins were visualized using the ECL system (GE Healthcare) and an LAS3000 imager (Fujifilm).

2.5. LacZ gene activation and cytotoxicity of Cre-expressing AdVs

The Hep-CALNLZ cells were cultured on collagen-coated, 96-well plates and infected with AdVs at various MOIs in four-fold serial dilutions. After 48 h, cytotoxicity assays were performed using the Cell Counting Kit-8 (Dojindo Molecular Technologies), according to the manufacturer's instructions. To detect *LacZ* expression, the cells were fixed with 4% paraformaldehyde in PBS for 10 min, washed with PBS, and incubated in X-Gal solution (5 mM potassium ferricyanide, 5 mM potassium ferrocyanide, and 2 mM $MgCl_2$ in PBS) containing 0.5 mg/mL 5-bromo-4-chloro-3-indolyl-β-D-galactopyranoside (X-Gal; WAKO Pure Chemicals) at 37 °C overnight.

2.6. Extraction of total RNA and quantification of Ad-pIX mRNA levels

The HepG2 cells were infected with the AdVs at an MOI of 100 and were harvested after 24 h. The CN2-29 transgenic mice were injected with the AdVs at a dose of 1.0×10^9 PFU and were sacrificed to obtain their liver samples after 12 h. Total RNA was extracted from the cells or mouse livers using the RNeasy Mini Kit (Qiagen) and RNase-free DNase (Qiagen). Reverse transcription was performed using the High Capacity cDNA Reverse Transcription Kit (Applied Biosystems). Copy numbers of the Ad-pIX cDNA were assessed by quantitative real-time detection polymerase chain reaction (RTD-PCR) with the specific probe AdIX-354-S25FT (5′-[FAM]-TCAGCAGCTGTTGGATCTGCGCCAC-[TAMRA]-3′); AdIX-327-S24 (5′-TTTGACCCGGGAACTTAATGTCGT-3′) and AdIX-387-R19 (5′-GGAGGAAGCCTTCAGGGCA-3′) were used as primers. The standard curve was generated using pAxEFLacZ. Analyses were conducted using an ABI PRISM 7700 Sequence Detection System with TaqMan Universal PCR Master Mix (Applied Biosystems).

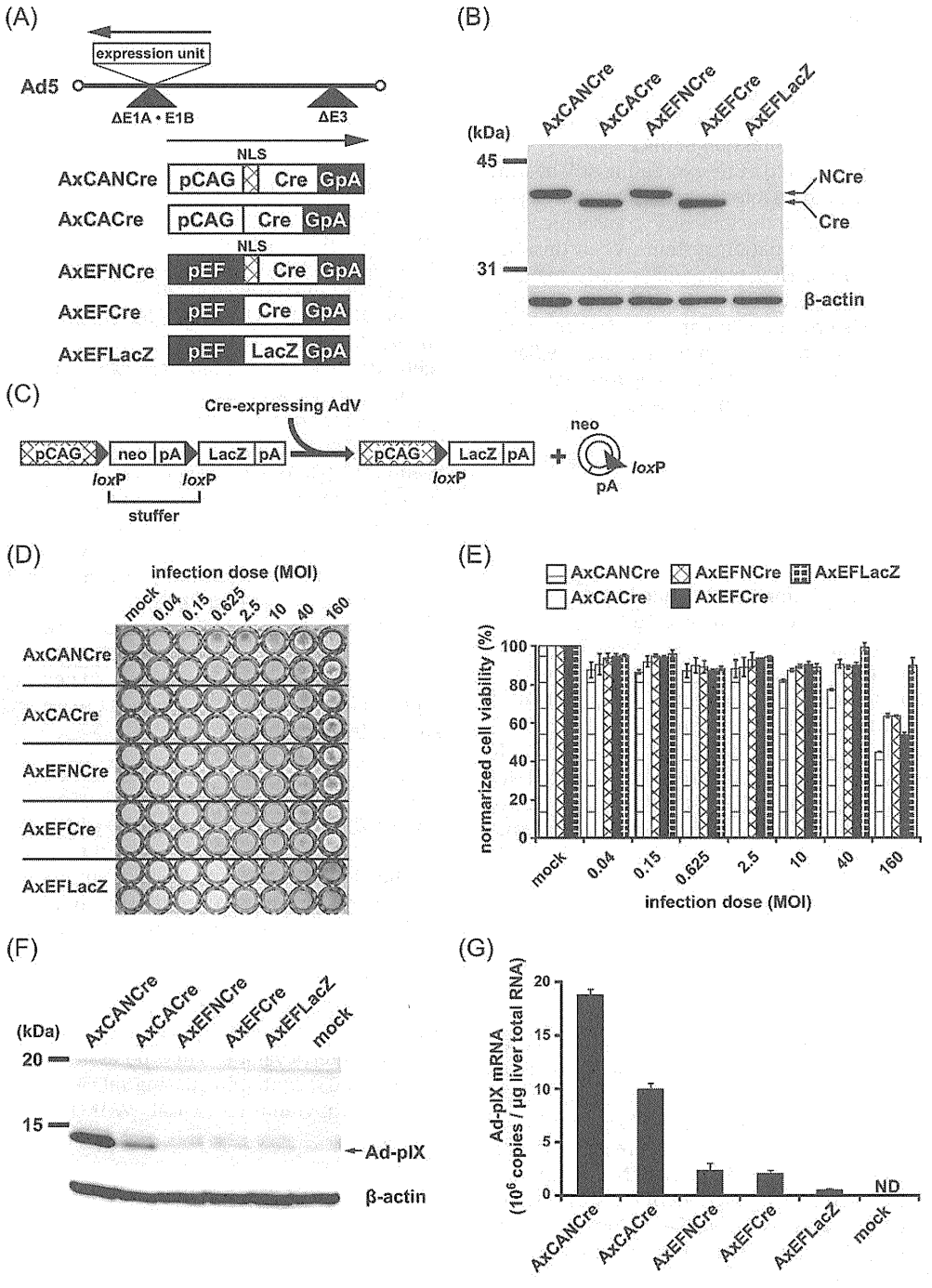

Fig. 1. Generation of AdVs expressing Cre under the control of different promoters. pCAG, CAG promoter; pEF, EF1α promoter; GpA, rabbit β-globin poly(A) signal; NLS, nuclear localization signal; neo, neomycin-resistance gene; pA, poly(A) signal; LacZ, β-galactosidase; Ad-pIX, adenovirus protein IX. (A) Structures of Cre-expressing AdVs. NLS-tagged Cre (NCre) or Cre were expressed under the control of the CAG or EF1α promoter. AxEFLacZ, which expresses LacZ under the control of the EF1α promoter, was used as a control. (B) Cre protein expression. HepG2 cells were infected with AdVs at an MOI of 20. After 24 h, total protein extracts from the cells were subjected to Western blotting. The detected β-actin protein is also shown. Note that mobility is slightly reduced when Cre is tagged with NLS (lanes, AxCANCre and AxEFNCre). (C) Schematic representation of *LacZ* transgene activation mediated by Cre-expressing AdV in Hep-CALNLZ cell chromosomes. Cre recognizes a pair of its target sequences *lox*P and removes the stuffer region as a circular DNA, resulting in expression of the transgene by the CAG promoter. (D) Cre recombination activity. Hep-CALNLZ cells were infected with Cre-expressing AdVs at the indicated dosages (four-fold serial dilutions; MOI range, 0.04–160). After 48 h, the cells were fixed and stained using X-gal staining. The first lane contains the mock-infected controls. The AxEFLacZ-infected lanes show the *LacZ*-gene-expressed control. (E) Cre cytotoxicities. Hep-CALNLZ cells were infected with AdVs at the indicated dosages (four-fold serial dilutions; MOI range, 0.04–160). After 48 h, cell viability was measured using a Cell Counting Kit-8. (F) Ad-pIX protein expression. HepG2 cells were infected with AdVs at an MOI of 100. After 24 h, total protein extracts from the cells were subjected to Western blotting. The detected β-actin protein is also shown. (G) mRNA expression of Ad-pIX. HepG2 cells were infected with AdVs at an MOI of 100. After 24 h, total RNA extracts from the cells were subjected to reverse transcription and quantitative RTD-PCR with an Ad-pIX-specific probe and a primer pair. ND, not detected.

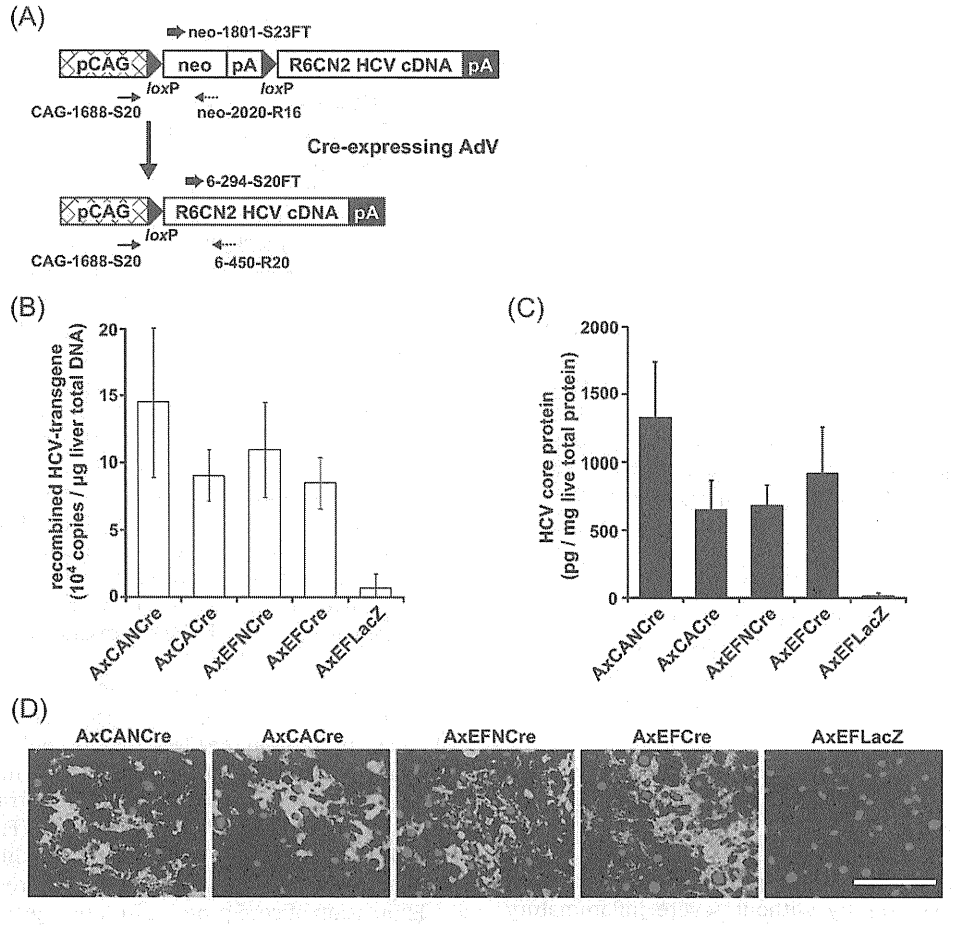

Fig. 2. Cre-mediated genomic DNA recombination and HCV core protein expression in transgenic mouse livers. (A) Structure of the Cre-mediated activation transgene unit CALNCN2 (Wakita et al., 1998). pCAG, CAG promoter; neo, neomycin-resistance gene; pA, poly(A) signal. The R6CN2 HCV cDNA (nucleotides 294–3435) contains the core, E1, E2, and NS2 regions. This construct does not allow HCV mRNA transcription prior to Cre-mediated DNA recombination, detected with the primer pair CAG-1688-S20 and neo-2020-R16. When Cre-expressing AdV is injected, the *neo* gene and poly(A) signal are removed by recombination between two *lox*P sequences. The recombined HCV transgene is detected with the primer pair CAG-1688-S20 and 6-450-R20. (B) Determination of Cre-mediated DNA recombination. CN2-29 transgenic mice were injected with 1.0×10^9 PFU for each AdV, and liver samples were harvested 7 days post-injection. Genomic DNA was extracted from the livers, and the numbers of copies of the recombined HCV-transgenes were determined using quantitative RTD-PCR with specific probes (6-294-S20FT) and a primer pair (CAG-1688-S20 and 6-450-R20). The values shown are means ± S.D. of more than three individual specimens. (C) Measurements of HCV core protein concentration in liver samples obtained from CN2-29 transgenic mice 7 days after injection of 1.0×10^9 PFU for each AdV. The samples were homogenized and the concentrations of HCV core protein were determined by EIA. The values shown are means ± S.D. of three individual specimens. (D) Immunofluorescence analysis of HCV core proteins. Liver sections of CN2-29 transgenic mice 7 days after injection of 1.0×10^9 PFU for each AdV were fixed and co-stained with rabbit anti-core polyclonal antibody (green) and DAPI (blue). Scale bar, 50 μm.

2.7. Determination of Cre-mediated HCV transgene recombination in mouse livers

The transgenic mouse livers were digested at 37 °C overnight in lysis buffer [50 mM Tris–HCl (pH 8.0), 0.1 M NaCl, 20 mM EDTA, 1% SDS] containing 1 mg/mL proteinase K. Total genomic DNA was then extracted using the phenol–chloroform extraction method. The copy numbers of the recombined HCV transgene in the livers were assessed via quantitative RTD-PCR (Takeuchi et al., 1999) with the specific probe 6-294-S20FT (5′-[FAM]-TGATAGGGTGCTTGCGAGTG-[TAMRA]-3′) and the primer pair CAG-1688-S20 (5′-GGTTGTTGTGCTGTCTCATC-3′) and 6-450-R20 (5′-ACAGGTAAACTCCACCAACG-3′) (Fig. 2A). The standard curve was generated using pCALNCN2/59-2 (Wakita et al., 1998) and quantitative RTD-PCR with the specific probe neo-1801-S23FT (5′-[FAM]-TCAAGAGACAGGATGAGGATCGT-[TAMRA]-3′) and the primer pair CAG-1688-S20 (5′-GGTTGTTGTGCTGTCTCATC-3′) and neo-2020-R16 (5′-TGCCTCGTCCTGCAGT-3′) (Fig. 2A). The *GAPDH* gene was used as an internal control for all samples. Analyses were carried out on an ABI PRISM 7700 Sequence Detection System with TaqMan Universal PCR Master Mix (Applied Biosystems).

2.8. Quantitation of HCV core proteins in mouse liver lysates

The transgenic mouse livers were homogenized in 0.5 mL RIPA buffer, and centrifuged at 15,000 rpm for 10 min at 4 °C. The protein concentrations of the supernatants were measured using the Bradford method (DC protein assay; Bio-Rad). The concentrations of HCV core proteins in the liver samples were determined using the Ortho HCV core protein ELISA kit (Eiken Chemical).

2.9. Biochemical analyses of mouse sera

Sequential blood samples were obtained by orbital bleeding after each AdV administration, and the sera were isolated by centrifugation at 10,000 rpm for 3 min at 4 °C. Serum ALT levels were determined using the Transaminase-CII Test A (Wako Pure Chemicals).

2.10. Histology and immunohistochemical staining

The liver samples were fixed with 4% paraformaldehyde in PBS, paraffin-embedded, sectioned at 4-μm thickness, and stained

with hematoxylin and eosin (H&E). Liver histology was evaluated according to modified Histology Activity Index (HAI) scores in three categories: piecemeal necrosis, spotty necrosis, and portal inflammation (Knodell et al., 1981; Yang et al., 1994).

The liver tissues were frozen in OCT compound (Tissue Tech) for immunohistochemical staining of HCV core proteins. The sections were fixed with a 1:1 solution of acetone:methanol at −20 °C for 10 min and then washed with PBS. Subsequently, the sections were incubated with the IgG fraction of an anti-HCV core rabbit polyclonal antibody (RR8) (Wakita et al., 1998) labeled with biotin in blocking buffer for 1 h at 4 °C. The sections were incubated with strept–avidin-conjugated horseradish peroxidase for 30 min at room temperature. Immunohistochemical staining was conducted using the Tyramide Signal Amplification Kit (Molecular Probes). Fluorescently labeled sections were stained with 4′,6-diamidino-2-phenylindole (DAPI; Molecular Probes) to stain the cell nuclei at room temperature before cover slipping. Fluorescence was observed under a fluorescence microscope (Carl Zeiss).

2.11. Statistical analysis

Data are shown as the mean ± S.D. Statistical analyses were performed using analysis of variance (ANOVA) followed by the Student–Newman–Keuls (SNK) test or analyzed using the unpaired Student's *t*-test. Statistical significance was established at $p < 0.05$.

3. Results

3.1. Generation of Cre-expressing AdVs

To enable HCV transgenic mice using the Cre/*lox*P system to express HCV protein persistently without severe inflammatory responses to AdV, we first constructed AdVs that expressed Cre with or without a nuclear localization signal (NLS) tag (AxEFNCre or AxEFCre, respectively) together with *LacZ* under the control of the EF1α promoter (AxEFLacZ) (Fig. 1A). AxCANCre and AxCACre were also generated to compare the impacts of using the CAG promoter and the EF1α promoter (Fig. 1A). Expression of Cre proteins from various AdVs was confirmed in human liver-derived HepG2 cells by Western blot analysis (Fig. 1B). Cre protein expression levels were not significantly different whether the gene was expressed under the control of the CAG or the EF1α promoter in the HepG2 cells (Fig. 1B). Next, we examined the recombination activities of Cre expressed via the AdVs using the Hep-CALNLZ cell line, HepG2 cells that express CALNLZ (Fig. 1C). When the Cre-expressing AdVs bearing the CAG or EF1α promoters infected these cells, the blue color produced by *LacZ* activation was observed for MOIs of 0.15–160. The cells infected with AxEFLacZ showed the blue staining in an MOI-dependent manner (Fig. 1D, lane AxEFLacZ). In contrast, the color faded for MOIs >40 when the Cre-expressing AdVs were used (Fig. 1D, lanes AxCANCre, AxCACre, AxEFNCre, and AxEFCre). At an MOI of 160, all of the Cre-expressing AdVs resulted in cytotoxicity, while the LacZ-expressing AdV did not affect cell viability (Fig. 1E).

AdV-induced immune responses are partly caused by co-expression of Ad-pIX (Nakai et al., 2007). To confirm the protein expression levels of Ad-pIX due to the AdVs, we performed Western blotting with anti-Ad-pIX sera (Fig. 1F). When HepG2 cells were infected with AdVs bearing the CAG promoter, significant amounts of Ad-pIX were detected as 14-kDa bands (Fig. 1F, lanes AxCANCre and AxCACre). In contrast, when using AdVs bearing the EF1α promoter, the 14-kDa band representing Ad-pIX was undetectable, as was the case for mock-infected HepG2 cells (Fig. 1F, lanes AxEFNCre, AxEFCre, AxEFLacZ, and mock). We also examined the mRNA expression levels of Ad-pIX and obtained similar results that correlated with the protein expression levels (Fig. 1G).

3.2. HCV gene expression and core protein production mediated by various Cre-expressing AdVs in transgenic mouse livers

The HCV transgenic mouse CN2-29 contains a reporter unit (CALNCN2) that is activated by Cre and conditionally expresses the HCV gene (Fig. 2A; Wakita et al., 1998). To assess the efficiency of Cre-expressing AdVs in promoting HCV gene expression, we intravenously injected the CN2-29 transgenic mice with various AdVs. At 7 days post-injection, Cre protein expression was confirmed by Western blot analysis of liver lysates (data not shown). The recombined HCV transgene levels in the livers were determined by quantitative RTD-PCR using specific probes and primer pairs, as described in Section 2 (Fig. 2A and B). When each Cre-expressing AdV was injected, the respective recombined HCV transgene was detectable; AxCANCre-injected CN2-29 transgenic mice expressed the highest levels of the recombined HCV transgene in their livers (Fig. 2B). CN2-29 transgenic mice injected with AdVs expressing NLS-tagged Cre had higher levels of the recombined HCV transgene in their livers (Fig. 2B, AxCANCre and AxEFNCre). This result suggests that NLS-tagged Cre efficiently translocated to the cell nucleus, which is consistent with our previous data (Baba et al., 2005). However, the levels of the recombined HCV transgene were not correlated with the expression level of HCV core protein (Fig. 2C).

The core protein levels in the livers were measured by enzyme immunoassay (EIA) as described in Section 2. The expression of the E1 and E2 proteins in the CN2–29 transgenic mouse livers has been shown previously (Wakita et al., 1998). The mean core protein level was 1.3 ng/mg total protein in the CN2-29 transgenic mouse livers 7 days after administration of AxCANCre (Fig. 2C). AxCACre- and AxEFNCre-injected mice expressed approximately one-half of the core protein levels resulting from AxCANCre injection (Fig. 2C).

Expression of core proteins in AdV-injected CN2-29 transgenic mouse livers was confirmed through immunofluorescence staining. Core proteins were expressed in the hepatocytes in the lobules of liver sections from Cre-expressing AdV-injected mice (Fig. 2D). In contrast, AxEFLacZ-injected transgenic mice did not express core proteins (Fig. 2C and D).

3.3. Liver injury and Ad-pIX expression in HCV transgenic mice injected with AdVs

To evaluate hepatocellular injury caused by expression of HCV proteins in CN2-29 transgenic mice injected with Cre-expressing AdVs, we serially estimated the serum ALT levels (Fig. 3A). For AxCANCre, the serum ALT level was elevated on day 5 and peaked 1–2 weeks post-injection (Fig. 3A, open triangle). ALT levels in AxCACre-injected transgenic mice were also elevated, although these levels declined over time (Fig. 3A, open circle). When AxEFNCre or AxEFCre was injected, ALT levels did not immediately increase, although they gradually increased after day 5 (Fig. 3A, closed triangle and closed circle, respectively). Injection of AxEFLacZ did not increase serum ALT levels in the CN2-29 transgenic mice (Fig. 3A, closed rectangle).

We also performed histological analyses of liver sections from CN2–29 transgenic mice 7 days after AdV injection (Fig. 3B). We found that severe inflammation with lymphocyte infiltration and spotty necrosis were diffusely observed in the livers of mice injected with the AdVs bearing the CAG promoter (AxCACre and AxCANCre) (Fig. 3B, a,b). In contrast, AxEFNCre-injected and AxEFCre-injected transgenic mouse livers exhibited mild inflammation without massive piecemeal necrosis on day 7 (Fig. 3B, c,d). No inflammation was observed in the AxEFLacZ-injected mice (Fig. 3B, e).

To confirm the expression levels of Ad-pIX in AdV-injected transgenic mice, we determined Ad-pIX mRNA in the liver using